



Scottish Universities Environmental Research Centre

**Characterising luminescence stratigraphies
in the Mount Elgon Caves
(Chepynalil rockshelter and Kiptogot Cave)**

Luminescence dating report

July 2014

T.C. Kinnaird¹, R.N. Kinyanjui², E.K. Ndiema²,
P. Powles, S.H. Powles, E.M. Walukana²,
P. Watene, T. Jovanelly³, P. Kiura¹,
D.C.W. Sanderson¹ and J.Q. Spencer⁴

¹SUERC, East Kilbride, Scotland, UK

²National Museums of Kenya, Nairobi, Kenya

³Berry College, Mount Berry, US

⁴Kansas State University, Kansas, US

East Kilbride Glasgow G75 0QF Telephone: 01355 223332 Fax: 01355 229898



The University of Glasgow, charity number SC004401



The University of Edinburgh is a charitable body,
registered in Scotland, with registration number SC005336

Summary

This report provides sediment-luminescence stratigraphies for key sedimentary sequences in the Chepnyalil and Kiptogot rockshelters, Mount Elgon, Kenya. Recent excavations in the two aforementioned caves by the National Museum of Kenya have unearthed lithic tool assemblages, which resemble both Middle Stone Age (MSA) and Late Stone Age (LSA) technologies (e.g. levallois and discol core reduction methods) and typologies (retouched points, bladelets, geometrics; Kiura, 2012). It should be noted that younger assemblages are also found. If the sediment-OSL chronologies reported herein confirm the MSA and LSA typological classification, and by association the implied occupation of the caves, then this provides the first evidence of MSA occupation in this topographically elevated region of East Africa. Furthermore, as environmental proxies indicate that the late Pleistocene to early Holocene was marked by increase aridity, it suggests an important link between the environment and human adaptations, as people moved from lowlands to higher elevation ecosystems. The above observations all stress the need for a detailed sediment-OSL chronology to determine TPQ and TAQ for occupational phases in the Mount Elgon caves, specifically at Chepnyalil and Kiptogot.

T. Kinnaird visited the Mount Elgon caves in October 2013 to collect samples for OSL profiling and dating. During fieldwork portable OSL equipment, in combination with field spectrometry, was used to appraise luminescence stratigraphies, and identify the key units for OSL dating. The field objective was to obtain luminescence proxy information from sediment stratigraphies at both Chepnyalil and Kiptogot, and assess this data against existing chronological data (including sediment depositional ages; 15-23 ka, and radiocarbon ages; 3rd - 15th century AD) to determine if maxima/trends in the profiles were suggestive of a prolonged environmental history, indicative of a multiphase occupational history. Sediment-OSL stratigraphies were generated for 8 profiles - 5 from Chepnyalil rockshelter and 3 from Kiptogot cave. The significance of these profiles is that they encompass strata (i) enclosing the lithic MSA?/LSA? typologies (profiles 1 and 2, Chepnyalil), and dated to 15-23 ka (profiles 1 and 2, Chepnyalil), and (iii) strata enclosing the younger occupational materials (profiles 3 and 4, Chepnyalil). Intriguingly, the field data did distinguish each stratigraphic unit, emphasising distinct luminescence packages/or units, and an overall progression in signal intensities with depth, consistent with at least a fourfold model of sediment accumulation. Moreover, through reference to the independent age controls, it was possible to assign discrete packages of sediment in the lower cave at Chepnyalil (Leopards Cave) and in the Kiptogot Cave to temporal units on the basis of their luminescence proxies. Field gamma dose rates were high, between 1.1 and 1.7 mGy a⁻¹, implying that high environmental dose rates would be encountered in the dating samples.

Laboratory profiling confirmed the correlations suggested in the field profiling dataset. Furthermore, the laboratory profiling results from the lower and upper units (i and ii, above) at Chepnyalil and Kiptogot, indicated a significant step in stored dose values across this lithological boundary (2-3 Gy vs 18 Gy and above), consistent with a notable unconformity, and the hypothesis that the caves have a prolonged, complex history of occupation. In addition, the calibrated luminescence screening results, indicated the dating samples which could be dated using the conventional quartz SAR

approach (the fast component of the quartz OSL signal will register stored doses up to 75-80 Gy, which in the Chepnyalil/Kiptogot environmental settings, is equivalent to 15-20ka), and those that would require higher temperature quartz approaches, and/or, post-IR elevated temperature IRSL protocols on K feldspar. Interestingly, the range in apparent stored dose estimates obtained for the stratigraphies at Chepnyalil and Kiptogot, in this environmental setting, corresponds to luminescence ages between 200 yrs BP and 25 ka BP, providing further confirmation of a prolonged environmental chronology, and suggesting a complex, multiphase occupational history.

Finally, quartz SAR OSL analyses, and preliminary K feldspar post-IR elevated temperature IRSL measurements, provide the means to construct sediment-OSL chronologies for the stratigraphies at Chepnyalil and Kiptogot. It must be noted that full quantitative luminescence dating was restricted to five samples. Four out of the five samples produced finite quartz SAR ages - 5.8 ± 0.4 ka (SUTL2613), 6.7 ± 0.4 ka (SUTL2620), 0.19 ± 0.01 ka (AD 1830 \pm 10, SUTL2626) and 4.6 ± 0.3 ka (SUTL2627). The fifth sample (SUTL2612) returned normalised OSL signals larger than the saturation limit of the dose response curve. A minimum age estimate of > 20 ka is suggested for this sample. The depositional ages reported here for Chepnyalil (SUTL2612 and 2613) verify that the lower units (in the position of profile 2), enclosing the lithic assemblages which resemble MSA and LSA technologies, do contain strata of LSA age (the LSA is subdivided into the Terminal Pleistocene, 40-12 ka, early Holocene, 12-8ka, middle Holocene, 8-4.5ka and late Holocene, 4.5-2ka). In contrast, the depositional ages from Kiptogot cave (SUTL2626 and 2627), do not yield LSA-equivalent ages; however, both the field and laboratory profiling datasets, do suggest that the sediment-OSL chronologies extend into the Pleistocene. At present work is underway to characterise the stability of the post-IR IRSL signals over prolonged periods of accumulation/storage; once complete, the report will be updated to include a post-IR IRSL age for SUTL2612.

Interestingly, the sediment-luminescence profiles, generated in the field and subsequently calibrated for sensitivities/age in the laboratory, together with the full quantitative luminescence dating analyses, have all verified a prolonged environmental temporal record for the sediments at Chepnyalil and Kiptogot, consistent with a complex, multi-period occupation of the caves.

Contents

Summary	i
1. Introduction	6
1.1. Background (Kiura, 2012)	6
1.2. Luminescence background	7
2. Sampling	9
3. Field Measurements	26
3.1. Dose rate measurements and determinations	26
3.2. Field luminescence measurements	26
4. Calibrated laboratory luminescence screening measurements	32
4.1. Methodology	32
4.2. Results	32
5. Quartz SAR/alkali feldspar SARA measurements	35
5.1. Sample preparation	35
5.1.1. Water contents	35
5.1.2. HRGS and TSBC Sample Preparation	35
5.1.3. Quartz/feldspar Sample Preparation	35
5.2. Measurements and determinations	36
5.2.1. Dose rate determinations	36
5.2.2. Exploratory quartz / feldspar SAR determinations	37
5.2.3. Exploratory feldspar SARA luminescence measurements	37
5.3. Results	38
5.3.1. Dose rates	38
5.3.2. Exploratory quartz / feldspar SAR screening measurements	40
5.3.3. Quartz SAR OSL determinations	42
5.3.1. Age determinations	45
6. Discussion and conclusions	45
7. Acknowledgements	48
8. References	48
Appendix A: Chemical analysis of soil samples from Chepnyalil cave	51
Appendix B: Luminescence Field Profiling Results	52
Appendix C: Calibrated luminescence screening measurements - composite dose response curves	54
Appendix D: Dose response curves	56

List of figures

Figure 2-1: Chenyalil Cave (a) Cave entrance from North; test-pit 1 was located in front of the two gentlemen; (b) excavation from north, NB: location of waterfall photograph left, and the spray-line within the cliff; (c) excavation from the south.....	10
Figure 2-2: Kiptogot Cave, illustrating the spatial distribution of the test-pit excavations.....	11
Figure 2-3: Profile 1, Test Pit 1, Chepnyalil Cave.....	19
Figure 2-4: Profile 2, Test Pit 1, Chepnyalil Cave.....	20
Figure 2-5: Profile 3, Test Pit 3, Chepnyalil Cave.....	21
Figure 2-6: Profile 4, Test Pit 2, Chepnyalil Cave Upper.....	22
Figure 2-7: Profile 6, Test Pit 1, Kiptogot Cave.....	23
Figure 2-8: Profile 7, Test Pit 3, Kiptogot Cave.....	24
Figure 2-9: Profile 8, Test Pit 2, Kiptogot Cave.....	25
Figure 3-1: Field profiles from Chepnyalil Cave. The profiles on the left are from the main cave; the lower profiles encompass strata which has been previously dated to 15-20ka (J. Spencer, pers com.); the upper profiles encompass strata which has been previously dated to the 15 th century (see table 1-1). The profile on the right is from the lower cave at Chepnyalil, the Leopards Cave. This profiles contains strata which has previously been dated to the 3 rd and 4th century AD.....	28
Figure 3-2: Field profiles from Kiptogot Cave.....	29
Figure 5-1: Composite dose responses for the IRSL signal at 50°C, and the equivalent MET post-IR IRSL signals at 200°C, 250°C and 300°C.....	41
Figure 5-2: Preheat plateaus for SUTL2613 and SUTL2627.....	42
Figure 5-3: Pulsed annealing plots for the K feldspars extracts from SUTL2439 and 2440.....	43
Figure 5-4: Pulsed annealing plots for the quartz extracts from SUTL2621 and 2623.....	43
Figure 5-5: Linearly-modulated (LM)-OSL curves obtained for sample SUTL2349, during natural readout, preheat, irradiation, and irradiation/preheat/readout cycles....	44

List of tables

Table 1-1: Age constraints obtained for the sediment stratigraphies at Chepnyalil Cave	6
Table 2-1: Field profiling sample locations, descriptions, and SUERC laboratory numbers;.....	14
Table 2-2: Laboratory profiling sample locations, descriptions, and SUERC laboratory numbers.....	15
Table 2-3: Dating sample locations, descriptions, and SUERC laboratory numbers ..	17
Table 2-4: Radiocarbon sample details/descriptions, samples assigned a GU number were submitted to the radiocarbon facilities at SUERC for dating, to provide an independent age constraint on the luminescence quartz/feldspar ages	18
Table 3-1: In situ gamma dose rates measurements made using a Health Physics Instruments Rainbow MCA with a 2"x 2" NaI probe.....	26
Table 4-1: Quartz (HF-etched) stored dose and sensitivity estimates obtained using a simplified two-step OSL SAR procedure	33
Table 4-2: Polymineral stored dose and sensitivity estimates obtained using a simplified two-step post-IRSL OSL SAR procedure.....	34
Table 5-1: Activity and equivalent concentrations of K, U and Th determined by HRGS.....	39
Table 5-2: Infinite matrix dose rates determined by HRGS and TSBC.....	39
Table 5-3: Water contents, and effective beta and gamma dose rates following water correction.	40
Table 5-4: Quartz OSL SAR /K feldspar IRSL SAR/post-IR IRSL at 300°C stored dose estimates	42
Table 5-5: Quartz SAR OSL quality parameters. Standard errors given.	45
Table 5-6: Total dose rates, stored dose and age estimates.....	45
Table 6-1: Independent age estimates for the sediment stratigraphies at Chepnyalil and Kiptogot, including new radiocarbon assays completed post-fieldwork	47

1. Introduction

This report is concerned with optically stimulated luminescence (OSL) investigations of a number of sediment stratigraphies within the Mount Elgon caves (Mount Elgon National Park, western Kenya), providing the chronological framework to interpret the alleged occupation of the caves from the Middle Stone Period to the present day. The caves in question are Kitum, Mackingeny, Ngwarisha, Kiptoro, Chepnyalil and Kipogot.

Preliminary surveys in the Kitum, Mackingeny, Kiptoro and Chepnyalil caves in 2009, followed by extensive excavations in Chepnyalil caves in 2010, identified a variety of lithic tools which resemble Middle Stone Age technologies (Kiura et al., 2013). The existing chronological evidence for Chepnyalil Cave indicates a long, protracted history of occupation, potentially with occupational phases in the Middle Stone Age, the Late Stone Age (c. 23.2 ± 2.4 ka; Table 1-1), the 3rd - 4th century AD, the 15th century AD, and at present.

Method	Locality	Sample no.	Context	Constraint
OSL	Chepnyalil, Upper Cave, Test Pit 1	Sample 2995	Level 99.89; 11 cm beneath ground surface	15.4 ± 4.1 ka (before 2011)
		Sample 2984	Level 99.26; 74 cm beneath surface	23.2 ± 2.4 ka
Radiocarbon	Leopard Cave, Test Pit 1	Beta-307191	45 cm beneath cave floor	1680 ± 30 yrs BP; cal AD 260-290 and 320-420
	Chepnyalil, Upper Cave, Test Pit 2	Beta-307192	Level 98.56; 141 cm beneath ground surface	480 ± 30 yrs BP; cal AD 1410 to 1450

Table 1-1: Age constraints obtained for the sediment stratigraphies at Chepnyalil Cave
OSL constraints – J. Spencer, reported informally to P.Powles, Radiocarbon assays- Beta Analytical

The aim of this investigation is to provide detailed chronologies for the sediment stratigraphies in the Chepnyalil and Kiptogot caves in support of the Museum of Kenya's archaeological investigations into the historic and prehistoric occupation. Specifically, it will establish sediment-OSL stratigraphies/chronologies for the multi-phase occupation of Chepnyalil and Kiptogot, to provide temporal constraints on the lithic-tool typologies, to test models of sediment accumulation and reworking of the sites, and provide independent controls on the ^{14}C results.

1.1. Background (Kiura, 2012)

Archaeological materials ranging from the Middle Stone Age to Late Stone Age technology have been recovered in many open and closed (caves) sites within the Rift Valley of Kenya, including Enkapune ya Moto and Kapthurin Formation. However most of MSA sites in Africa are in South Africa and include Howiesons Poort, Peers Cave, Diepkloof, Border Cave, Rose Cottage, Nelson Bay Cave, Klasies River Mouth, Uhmlatuzana, Boomplas and Apollo II.

The technological transition between the MSA and LSA is marked by flake-based stone tool industries made on radial and levallois cores with prepared platforms in the

MSA and replaced by blade and small flake-based industries usually made from core with plain platforms in the LSA and UP. Most of the tools within the LSA are made of fine grained raw materials and include chert and obsidian.

The excavations at Chepnyalil and Kiptogot have unearthed lithic tool assemblages (n= 1102 and 1370, respectively) which resemble MSA technologies, both levallois and discoi core reduction methods, and typologies e.g. retouched points. In addition, the lithic assemblage also features commonly found in the LSA, such as bladelets. If the sediment-OSL chronologies reported herein confirm the MSA and LSA occupations, then this indicates that the Mount Elgon caves contain one of the earliest enclosed (cave) sites of human occupation in East Africa. Furthermore, environmental proxies suggest that the Pleistocene to early Holocene was marked by increase aridity, and if the age associations are verified by OSL dating, then this suggests an important link between environment and human adaptations, as the MSA/LSA populations moved to higher elevation ecosystems.

The above observation all stress the need for a detailed sediment-OSL chronology to determine TPQ and TAQ for the occupational phases in the Mount Elgon Caves, specifically at Chepnyalil and Kiptogot.

1.2. Luminescence background

Optically stimulated luminescence originates as a consequence of energy deposited within sedimentary minerals in response to naturally occurring ionising radiation in the sample and its environment. By stimulating the minerals in the laboratory using lasers or other suitable light sources, part of this stored energy is released, resulting in luminescence which can be measured to quantify the radiation history of the sample. Luminescence signals can be erased either by heat or exposure to daylight, and for sedimentary materials exposure to light during erosional or transport phases acts as the zeroing mechanism. Enclosure of the sediment after final deposition protects it from light and allows the accumulation of luminescence signals that can be used for age estimation. The luminescence age is determined by combining luminescence determinations of the radiation dose equivalent to the signals recovered from the samples (the equivalent dose), with measurements of the radiation dosimetry of the sample and its environment (the dose rate). The natural dose rate comprises alpha, beta and gamma radiation produced by the decay of naturally occurring radionuclides (^{40}K , and the U and Th decay series), and cosmic radiation. The luminescence age is the quotient of equivalent dose over dose rate.

With sediment dating it is important to recognise that the luminescence age might represent an accumulated signal originating from many cycles of erosion, transport, bleaching and deposition. Only in the situation where undisturbed sediments are available and associated with effective zeroing at time of deposition can sediment dates be interpreted in terms of simple events. It is also important to recognise that the dose rate values used for age estimation are based on contemporary measurements of the sample and its environment. These must be spatially representative, and expected variations in dose rate to the sample with time must be accounted for. Water absorbs radiation, so average water content during burial is estimated using the sample's water retention properties and by modelling its hydrological history. Gross precipitation or

leaching of radionuclides can be detected using gamma spectrometry, while the effects of bulk mineral precipitation (e.g. carbonates), which may be accompanied by U series mobilisation and disequilibrium, may require modelling based on the expected age of the precipitate.

In much luminescence dating work quartz is used as the primary dosimeter (Huntley et al., 1985; Murray and Wintle, 2000), with the initial part of the OSL signal, the “fast” component (Bailey, 1998) used in age determination. This part of the signal is known to show little growth with dose when samples are irradiated above a few hundred Gy. This therefore limits the dating range of quartz using conventional techniques. To extend the working dose range of quartz, one must examine other parts of the luminescence signal. One approach is TT-OSL (Pagonis et al., 2008; Tsukamoto et al., 2008; Wang et al., 2006) which examines signals associated with deeper ‘source-traps’ (Adamiec et al., 2008; Adamiec et al., 2010) which can be thermally transferred into ‘OSL’ traps prior to OSL readout. The saturation levels, thermal stability and sensitivity to bleaching of the TT-OSL signal thus reflect the characteristics of such deeper source traps (see review in Duller and Wintle, 2011).

Luminescence signals from feldspars continue to grow to far higher doses than those from quartz; this offers the possibility of dating significantly older material providing sufficiently stable signals can be achieved. The IRSL and TL signals from feldspars are expected to respond to additional radiation up to the 1 – 5 kGy range. In a low dose rate environment, this means that there is the potential to date sediments well beyond ~ 250 ka. Unfortunately, the luminescence signals from feldspar may fade at a rate faster than expected simply from a consideration of trap depth and ambient temperature (a phenomenon termed ‘anomalous fading’ by Wintle, 1973). Some authors (Huntley and Lamothe, 2001; Spooner, 1992) have suggested that anomalous fading is inherent to some extent within all feldspars. However in practice, signal stability is dependent on the mineralogy of the studied feldspar (Alexander, 2007; Krbetschek et al., 1997; Krbetschek and Rieser, 1995), its geological origins (Huntley and Lamothe, 2001; Zink et al., 1995), its structural configuration (i.e. order vs disorder; Visocekas et al., 1994; Visocekas et al., 1998), and its composition (i.e. major or minor element chemistry; Huntley, 2006; Huntley et al., 2007; Spooner, 1994). In addition, as thermal fading processes are always present, regardless of whether additional proximity or tunnelling effects are also operating, this will influence storage/accumulation temperatures and timescales (Sanderson, 1988a). Recent work (Buylaert et al., 2009; Thomsen et al., 2008) has suggested a new procedure based on elevated temperature post-IR IRSL measurements which can potentially produce the desired low fading rates under convenient automated conditions. They interpreted the increased signal stability of these post-IR IRSL as a consequence of the removal of unstable donor-acceptor pairs in close lattice proximity to each other during the prior IR stimulation at 50°C. In this explanation the subsequent post-IR IRSL signal is interpreted as originating in more distant pairs, which can be accessed by re-stimulating the sample at elevated temperatures. Recently, following Murray et al. (2009)’s study on preheat dependence and equivalent dose determination, Thiel et al. (2011) proposed post-IR IRSL stimulation at significantly higher temperatures to obtain higher signal intensities.

Kinnaird et al. (2012) examined the luminescence characteristics of sediment from Chepnyalil Cave. Their preliminary analyses (i) verified the presence of both quartz and K feldspar (see also, the chemical analysis of soil samples from Chepnyalil, by the Department of Mines and Geology, University of Nairobi, Appendix A); (ii) confirmed that the Chepnyalil quartz is dominated by the fast component, and this component is thermally stable; (iii) determined that the saturation limit of the conventional OSL signal is in the range 75 - 100 Gy, thereby, limiting the dating range of the conventional SAR protocol to 15 - 20 ka; (iv) identified that high-temperature quartz approaches and post-IR elevated temperature signals from feldspar provide alternative means of dating the older sediment from the Chepnyalil Cave; and that (v) the TT-OSL and post-OSL TL signals from quartz, and the post-IR IRSL signal from K feldspar, exhibit both higher saturation levels and greater thermal stability than OSL/IRSL. In summary, the preliminary investigations have established that the quartz OSL method will register dates up to 20 ka, and that the higher temperature methods are valid for longer timescales. Therefore, a first objective is to establish the preliminary age ranges of the dating samples, such that the most suitable dating protocol can be chosen.

2. Sampling

Tim Kinnaird visited the Chepnyalil rock shelter (Fig. 2-1) and Kipogot cave (Fig. 2-3) in October 2013, with the aim of collecting samples from key stratigraphic units for OSL dating. During fieldwork portable OSL equipment, in combination with field spectrometry, was used to appraise luminescence stratigraphies, and identify the key units for dating. Profiles 1-8 were taken by T.C. Kinnaird and/or R.N. Kinyanjui on visits to the caves between the 11 and 16th October 2013. 76 field profiling samples, 18 laboratory profiling samples, and 12 full dating samples were collected through 8 profiles. Profiles 1- 4 were taken through sediment stratigraphies in the main Chepnyalil rock shelter, profile 5 from a lower cave at Chepnyalil (henceforth Leopards cave), and profiles 5 – 8 from Kipogot cave.

The Chepnyalil rock shelter, located on the eastern flank of Mount Elgon, at an elevation of 2500m, is a small wide cave, about 26 m × 54 m wide. A central rock pillar (shown in Fig 2-1), fallen from the roof, separates the cave into two chambers, henceforth designated the northern and southern chambers. Test pits excavated and backfilled in 2010, were re-excavated and the sections cleaned back to facilitate further sample collection. In the lower Chepnyalil caves, fresh test-pits, measuring 1 × 1 m in dimension, were cut, to provide access to additional sediment stratigraphies. The excavations were conducted in 10 cm spits. Luminescence profiling samples were taken by first excavating the sections back to remove material which had been light exposed. Small quantities of sediment, weighing approximately 10g samples were recovered, and placed in a numbered petri dish for use with the portable OSL reader. These samples were sealed in labelled zip-seal bags and then placed in an opaque bag to protect them from further light exposure. The profiling samples were measured on-site using a SUERC portable OSL reader (Sanderson and Murphy, 2010) to provide initial observations of the luminescence signals in each stratigraphic sequence. Full luminescence dating samples were taken from the cleaned sections using stainless steel tubes (recovering ~200g of sediment). Field gamma spectrometry measurements were recorded in situ in close association to the dating samples. In addition, 'bulk'

quantities of sediment were recovered from around the dating positions for additional dosimetry measurements.



Figure 2-1: Chenyalil Cave (a) Cave entrance from North; test-pit 1 was located in front of the two gentlemen; (b) excavation from north, NB: location of waterfall photograph left, and the spray-line within the cliff; (c) excavation from the south.

Photographs courtesy of Peter Powles.



The profiles at Chepnyalil were selected to encompass the entire range of natural and archaeological sediments, from the basal clays which directly overlie bedrock to the modern materials forming the present floor of the cave. Test pit 1, measuring 2×2 m, is situated at the NNW entrance to the cave, at a ‘natural’ rise in the floor of the cave. Profiles 1 and 2 are located in this the main test pit: with 23 profiling samples covering the primary substrate (P1/10-P1/9; P2/13-P2/12; Figs 2-3 & 2-4; Table 2-1), the lower and upper archaeological materials (P1/8-P1/4; P2/11-P2/4), and the finer fill representing natural sedimentation after occupation (P1/3-P1/1; P2/3-P2/1). A total of 1445 specimens were collected from this test pit, of which 76.2% were lithic artefacts, 23.7% were faunal remains, and 0.6% were ceramic vestiges (Kiura, 2012). Joel Spencer, of Kanvas State University, obtained OSL ages of 15.4 ± 4.1 yrs BP and 23.2 ± 2.4 yrs BP, for strata at 99.89 and 99.26 m, respectively (Table 1-1). Samples for OSL profiling and dating were taken at strategic positions through profile 2, providing TPQ and TAQ on the age of the artefact-bearing horizon (Tables 2-2 and 2-3, respectively).

Test pit 2, measuring 2×1m, is located in a central position within the northern chamber. The sample set includes, from base to top, a basal clayey loam (P4/11; Fig. 2-6), archaeological materials enclosing a lower ash horizon (P4/10-P4/7), re-deposited gravels (P4/6), fines (P4/5-P4/3), a burnt, reddened horizon with associated ash (P4/2), and the modern materials forming the cave floor (P4/1). A charcoal fragment recovered from a depth of 0.4 m in the profile returned a radiocarbon age of 480 ± 30 yrs BP (Beta-307192; Table 1-1). Test pit 3, measuring 1×0.5m, is located in a central position within the southern chamber. Profile 3 was taken through this sediment stratigraphy, with samples collected from the basal clay (P3/8-P3/7; Fig. 2-5), the overlying archaeological fills (P3/6-P3/2), including burnt, reddened soils and ash (P3/3-P3/2) into the modern materials forming the cave floor (P3/1).

The profile at Leopards Cave (or lower Chepnyalil Cave) potentially encloses sediment related to the early occupation of the main rock shelter, and the later periods; the profile cuts 1.2 m of sediments, through poorly consolidated loams, to compacted red-brown clays, then bedrock. Profiling samples were collected at 10 cm intervals.

The Kiptogot rock shelter, located N of Chepnyalil but at a similar elevation, is a small wide cave, X×X wide (Fig. 2-2). Preliminary archaeological investigations were undertaken through a series of test-pit excavations during the first authors visit to the site in October 2013.

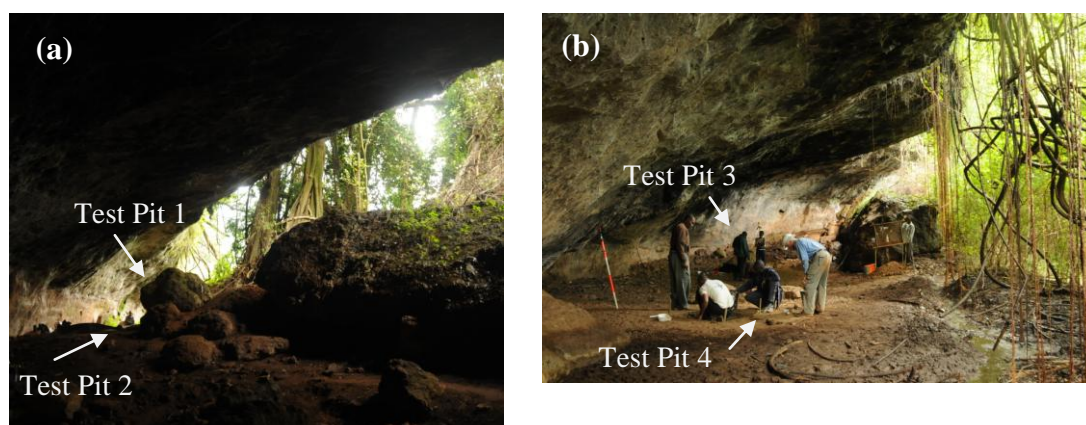


Figure 2-2: Kiptogot Cave, illustrating the spatial distribution of the test-pit excavations.
Photographs courtesy of Stephen Powles.

Test pit 1 was located at the eastern entrance to Kiptogot Cave (Fig 2-2a). Test pit 2 was located at the natural restriction between the rockshelter and fallen blocks (Fig 2-2a, several metres east of the rise indicated by the arrow). In contrast, test pits 3 and 4 were located in the main antechamber in front of the enclosed cave entrance; test pit 3 is located in close proximity to the outer rim of fallen blocks, slightly to the east of the entrance; whereas test pit 4 is located in the centre of the main antechamber. Again, samples were collected to encompass the full sequence of natural and archaeological fills, from the basal clays which directly overlie bedrock (or fallen blocks) to the modern materials forming the present cave floor. Profile 6, taken through the sediment pile in test-pit 1 (Fig. 2-7), encompasses all sediment between bedrock and the present cave surface, including sediment enclosing lithic tools of indeterminable age. Profiles 7 and 8 are located in the main antechamber, in front of the entrance to the internal

enclosed cave (which contains evidence of recent use), in test-pits 2 and 3 respectively (Figs 2-8 & 2-9). The two profiles share a common sedimentary sequence: from the base up, poorly consolidated red-brown clayey loams, enclosing chert/quartzite stone tools, through compacted, well consolidated red-brown clays enclosing quartz stone tools, to grey, poorly consolidated, dry loams forming the present cave floor. The profiles therefore potentially contain a record of several occupational phases, and thus, span a considerable amount of time.

Sampling details, including the labels assigned to each tube and bulk sample in the field, and the laboratory (SUTL) numbers assigned to each upon arrival at the SUERC luminescence dating laboratory, are summarised in Tables 2-1 to 2-4.

Field no.	DD	Description	Comments	
Profile 1: Chepnyalil Cave, Upper Level; Test Pit 1 (SUERC samples)				
P1/1	99.69*	brown, loamy topsoil	this profile is taken through the sediment pile thought to enclose artifacts attributed to the Middle Stone Age; the profile encloses the sediments sampled by Purity Kuira, and analysed at SUERC in 2012.	
P1/2	99.68			
P1/3	99.60	red-brown, compacted clayey loam		
P1/4	99.54			
P1/5	99.49			
P1/6	99.40			
P1/7	99.33			
P1/8	99.29			
P1/9	99.20			
P1/10	99.16			
Profile 2: Chepnyalil Cave, Upper Level; Test Pit 1 (Spencer samples)				
P2/1	99.97*	brown, loamy topsoil	this profile is taken through the sediment pile thought to enclose artifacts attributed to the Middle Stone Age; the profile encloses the sediments sampled by Purity Kuira, and analysed at Kansas State University in 2011; Joel Spencer (pers com.) obtained OSL ages at 99.89 99.26 of 15.4 ± 4.1 ka (before 2011) and 23.2 ± 2.4 ka, respectively	
P2/2	99.93			(=P2/1)
P2/3	99.88	red-brown, compacted clayey loam		
P2/4	99.83			(=OSL2)
P2/5	99.79			(=P2/2)
P2/6	99.73 99.68			(=OSL3)
P2/7	99.61			(=P2/3)
P2/8	99.55			(=OSL4)
P2/9	99.50			
P2/10	99.47			
P2/11	99.45			
P2/12	99.40			
P2/13	99.39			
Profile 3: Chepnyalil Cave, Upper level, 'southern' chamber; Test Pit 3				
P3/1	0.05†	grey fine-grained loam, topsoil; overlying ash horizon	this profile encompasses sediment associated with the most recent occupational phases of the cave, potentially from the present day, back till the mid 15 th century	
P3/2	0.10	reddened sediment; beneath ash horizon		
P3/3	0.15	red-brown clayey loam		
P3/4	0.20			
P3/5	0.25	tan-brown clayey soil		
P3/6	0.30			
P3/7	0.35	brown-grey clayey soil		
P3/8	0.45			
Profile 4: Chepnyalil Cave, Upper level, 'northern' chamber; Test Pit 2				
P4/1	99.97*	Topsoil	this profile encompasses sediment associated with the most recent occupational phases of the cave, potentially from the present day, back till the mid 15 th century; charcoal collected at a depth of 1.4m within this profile returned an age of 480 ± 30 yrs BP; cal AD 1410 to 1450	
P4/2	99.91	reddened sediment		
P4/3	98.86	brown clayey loam, containing small sub-angular clasts of local lithologies		
P4/4	98.82			
P4/5	98.79	brown clayey loam, immediately above pebble horizon		
P4/6	98.65			
P4/7	98.61	(= Beta-307192) clayey loam, beneath pebble horizon/above ash		
P4/8	98.56			
P4/9	98.52			
P4/10	98.48			
P4/11	98.41	Pinkish clayey loam		

Profile 5: Leopards Cave (Lower Chepnyalil Cave); Test Pit 1			
P5/1	0.10†	<p>Test pit 1 is located in lower Chepnyalil Cave (Leopards Cave). The test pit cuts through a 1.2 m thick sequence of sediments, from poorly consolidated loams at the top, to compacted red-brown clays at the base; it therefore potentially encompasses sediments deposited during the recent occupation of the upper cave, to sediments deposited at ~20ka.</p> <p>A radiocarbon age of 1680 ± 30 yrs BP (cal AD 260-290 and 320-420) was obtained from charcoal recovered at a depth of 0.45 m within this pit.</p>	
P5/2	0.20		
P5/3	0.30		
P5/4	0.40		
P5/5	0.50		
P5/6	0.60		
P5/7	0.70		
P5/8	0.80		
P5/9	0.90		
P5/10	1.00		
P5/11	1.10		
P5/12	1.20		
Profile 6: Kiptogot Cave; Test Pit 1			
P6/1	100.32	Surface, quartz and bone	<p>Test pit 1 is located at eastern entrance to Kiptogot Cave (access to the south is restricted due to fallen blocks); The profile encompasses all sediment between the present cave floor surface, and bedrock (or fallen block?) at 99.67m</p>
P6/2	100.22	between 100.15 and 100.25, quartz	
P6/3	100.12	stone tools	
P6/4	100.02		
P6/5	99.92		
Profile 7: Kiptogot Cave; Test Pit 2			
P7/1	99.70	<p>Test Pit 2 is located several metres west of test pit 1, in a sheltered position between the northern wall of the rock shelter, and the southern fallen blocks; it is located several metres east of the main cave entrance; This profile is taken through a stack of poorly consolidated grey and red-brown loams, artifact barren, before passing through a red-brown clayey loam, containing chalcedony and quartz stone artifacts, and the lowermost unit of compacted red-brown clays, containing quartz stone tools. It therefore potentially contains a record of several occupational phases, spanning a considerable amount of time.</p>	
P7/2	99.67		
P7/3	99.61		
P7/4	99.56		
P7/5	99.51		
P7/6	99.42		
P7/7	99.31		
P7/8	99.15		
P7/9	99.03		
P7/10	99.87		
Profile 8: Kiptogot Cave; Test Pit 3			
P8/1	97.30	<p>Test pit 3 is located in the main antechamber forward of the entrance to Kiptogot cave, several metres east of test pit 2. The section includes strata forming the present cave floor, and the underlying sequence of poorly consolidated red-brown clayey loams, enclosing chert/quartzite stone tools, and the compacted, well-consolidated red-brown clays, enclosing quartz stone tools. It therefore potentially contains a record of several occupational phases, spanning a considerable amount of time</p>	
P8/2	97.25		
P8/3	97.20		
P8/4	97.15		
P8/5	97.10		
P8/6	97.05		

Table 2-1: Field profiling sample locations, descriptions, and SUERC laboratory numbers; DD = Distance from datum, *Height from site datum, †Depth from cave floor

SUTL no.	Equivalent field profiling sample	HOD	Equivalent dating sample	Description	Significance
<i>Chepnyalil Cave; Test Pit 1 (equivalent to Profile 2)</i>					
2597A	P2/2	99.90	profiling samples bracket full dating samples	Grey, loamy material	the section encompasses the upper fill of the cave, potentially time-equivalent to the strata preserved in test pit 2, and the lower clayey horizons, enclosing stone finds attributed to the Middle Stone Age
2597B	P2/5	99.75		Red-brown, clayey loam, enclosing stone artifacts	
2597C	P2/7	99.68		Red-brown, clayey loam, although with no finds	
<i>Kiptogot Cave; Test Pit 2 (equivalent to Profile 7)</i>					
2598A	P7/1	99.70	-	Unit 1; brown-grey loam	the section encompasses the late and early occupational phases of the cave, as indicated by bronze and stone tool finds
2598B	P7/2	99.65	=P7/OSL1		
2598C	P7/5	99.48	=P7/OSL2	Unit 3; brown to red-brown, clayey loam	
2598D	P7/8	99.15	=P7/OSL3	Unit 4; red-brown clay; consolidated	
2598E	P7/10	98.55	-		
2598F	-	97.57	-		
<i>Kiptogot Cave; Test Pit 3 (equivalent to Profile 8)</i>					
-	P8/1	97.30	-	Modern materials	the section encompasses the late and early occupational phases of the cave, as indicated by bronze and stone tool finds
2599A	P8/2	97.25	-	Grey, loamy material; enclosing chert/quartzite/obsidian stone tools	
2599B	P8/3	97.20	=P8/OSL1		
2599C	P8/4	97.10	=P8/OSL2	Consolidated, compacted red-brown clay; enclosing quartz stone artifacts	
2599D	P8/5	97.00	-		
2599E	P8/6	96.90	-		

Table 2-2: Laboratory profiling sample locations, descriptions, and SUERC laboratory numbers

HOD = Height above site datum, except when marked by *, when value indicates depth beneath cave floor in m

SUERC no.	Field no.	HOD	Context	Description	Significance
<i>Chepnyalil Cave; Test Pit 1 (equivalent to Profile 2)</i>					
2612	P2 OSL1	100.29	Unit 1	Grey, loamy material	Provides a constraint on the age of the upper depositional unit; and terminus ante quem for stone artifact bearing horizon
2613	P2 OSL2	99.84	Unit 2	Red-brown, clayey loam, enclosing stone artifacts	Provides a constraint on the age of the stone artifact-bearing horizon
2614	P2 OSL3	99.68	Unit 3	Red-brown, clayey loam, although with no finds	Provides terminus post quem for the sediment enclosing the stone artifact bearing horizon
2615	P2 OSL4	99.57	Unit 3		Provides an age constraint on first sediment to be deposited within the cave
<i>Leopard Cave (Lower Chepnyalil Cave); Test Pit 1 (equivalent to Profile 5)</i>					
2616	P5 OSL1	0.42*	Unit 1, above ash	Charcoal at 50 & 55cm	
2617	P5 OSL2	0.70*	Unit 2, beneath ash		
2618	P5 OSL3	0.92*			
<i>Leopard Cave (Lower Chepnyalil Cave); Test Pit 2 (sampled 30/10/13)</i>					
2619	OSL1	0.50*		Red-brown, clayey loam; immediately above stoney horizon	Provides terminus ante quem on the age of the stone artifact-bearing horizon
2620	OSL2	1.00*		Stoney horizon; enclosing stone artifacts, obsidian and bone	Provides an age constraint on the first sediment to accumulate in this part of the cave; additionally constrains age of artifact-bearing horizon
<i>Kiptogot Cave; Test Pit 2 (equivalent to Profile 7)</i>					
2621	P7 OSL1	99.62	Unit 2	Brown-tan loam, poorly consolidated, contains sub-angular pebbles of local bedrock (<15mm)	Provides a temporal constraint to interpret the most recent phase of occupation of the cave; a temporal marker to interpret the field profiles; and terminus post quem for the age of the underlying stone artifact-bearing horizon
2622	P7 OSL2	99.57	Unit 3	Brown to red-brown, clayey loam; enclosing chalcedony/quartz stone artifacts; erosional contact with Unit 4	Provides an age constraint on the sediment enclosing the upper stone artifact bearing horizon
2623	P7 OSL3	99.11	Unit 4	Consolidated, compacted red-brown clay; enclosing quartz stone artifacts	Provides an age constraint on the sediment enclosing the lower stone artifact bearing horizon; and terminus post quem for the upper artifact-bearing horizon
<i>Kiptogot Cave; Test Pit 3 (equivalent to Profile 8)</i>					
2624	P8 OSL1	97.16	-	Grey, loamy	Provides an age constraint on the

				material; enclosing chert/quartzite/obsidian stone tools; (=8/3)	sediment enclosing the upper stone artifact bearing horizon
2625	P8 OSL2	97.08	-	Consolidated, compacted red-brown clay; enclosing quartz stone artifacts (=8/4)	Provides an age constraint on the sediment enclosing the lower stone artifact bearing horizon
<i>Kiptogot Cave; Test Pit 4 (sampled 28/10/13)</i>					
2626	P9 OSL1	97.16	-		
2627	P9 OSL2	97.08	-		

Table 2-3: Dating sample locations, descriptions, and SUERC laboratory numbers
HOD = Height above site datum, except when marked by *, when value indicates depth beneath cave floor in m

Date	SUERC ref	Test Pit	Depth	Description
<i>Leopard Cave (Lower Chepnyalil Cave); 'test pit 2'</i>				
30/10/2013	-	2	0.80 to 1.00	charcoal
30/10/2013	SUERC51768 (GU33321)		1.20 to 1.40	charcoal
<i>Leopard Cave (Lower Chepnyalil Cave); 'Sub-cave'</i>				
29/10/2013	-	sub-cave	0.25 to 0.30	Find no. 1: ash, from top of layer
29/10/2013	-		0.25 to 0.30	Find no. 1: ash, from bottom of layer
29/10/2013	-		0.30	Find no. 2: charcoal
29/10/2013	-		0.30	Find no. 2: coal?
<i>Leopard Cave (Lower Chepnyalil Cave); '2nd waterfall pit'</i>				
29/10/2013	-	2 nd waterfall cave	0.40	charcoal
29/10/2013	-		0.50	burnt pottery?
29/10/2013	SUERC51772 (GU33322)		0.55	charcoal, from top of burnt horizon
29/10/2013	-		0.55	charcoal, from base of burnt horizon
29/10/2013	-		0.70	charcoal
<i>Kiptogot Cave</i>				
21/10/2013	(GU33319)	4b	96.67	charcoal, site coordinates N991.49, E-967.54
21/10/2013	SUERC51767 (GU33320)	4c	97.00	charcoal, site coordinates N992.85, E967.45
21/10/2013	-	4d	96.76	charcoal, site coordinates N993.12, E967.10

Table 2-4: Radiocarbon sample details/descriptions, samples assigned a GU number were submitted to the radiocarbon facilities at SUERC for dating, to provide an independent age constraint on the luminescence quartz/feldspar ages



Figure 2-3: Profile 1, Test Pit 1, Chepnyalil Cave. The positions of the two full dating samples collected by Purity Kiura in 2011 are shown.

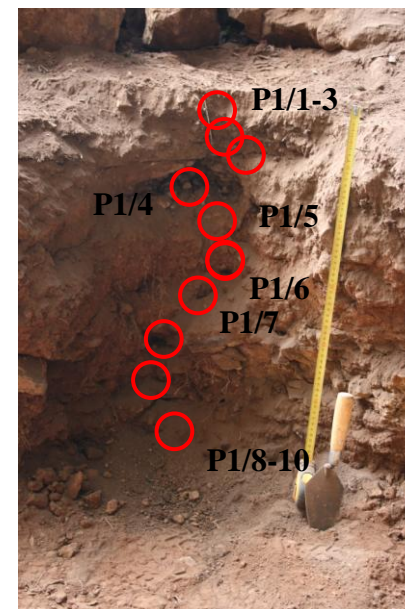




Figure 2-4: Profile 2, Test Pit 1, Chepnyalil Cave



Figure 2-5: Profile 3, Test Pit 3, Chepnyalil Cave
The positions of the field profiling samples are marked

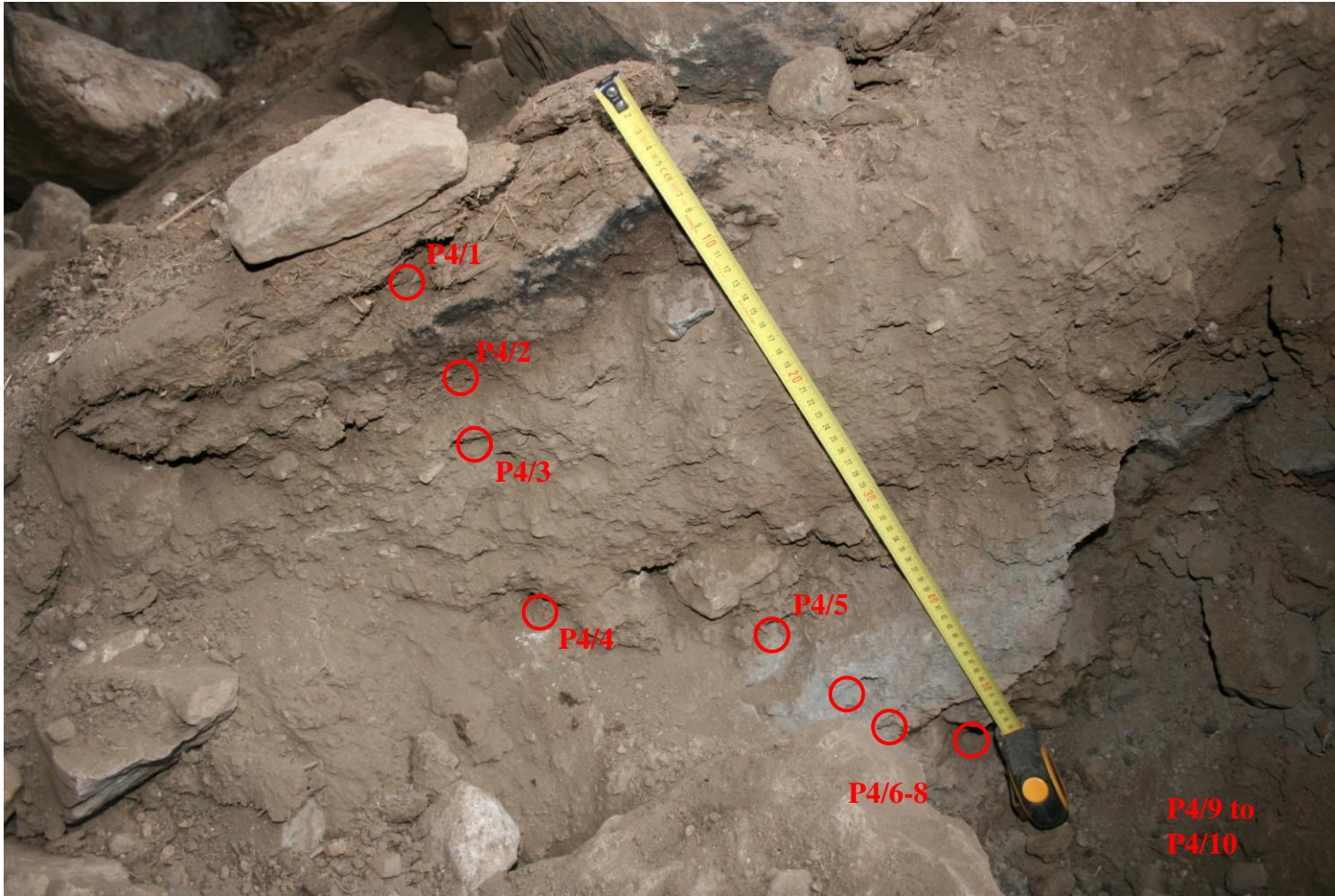


Figure 2-6: Profile 4, Test Pit 2, Chepnyalil Cave Upper
The positions of the field profiling samples are shown.



Figure 2-7: Profile 6, Test Pit 1, Kiptogot Cave.
The positions of the field profiling samples are shown

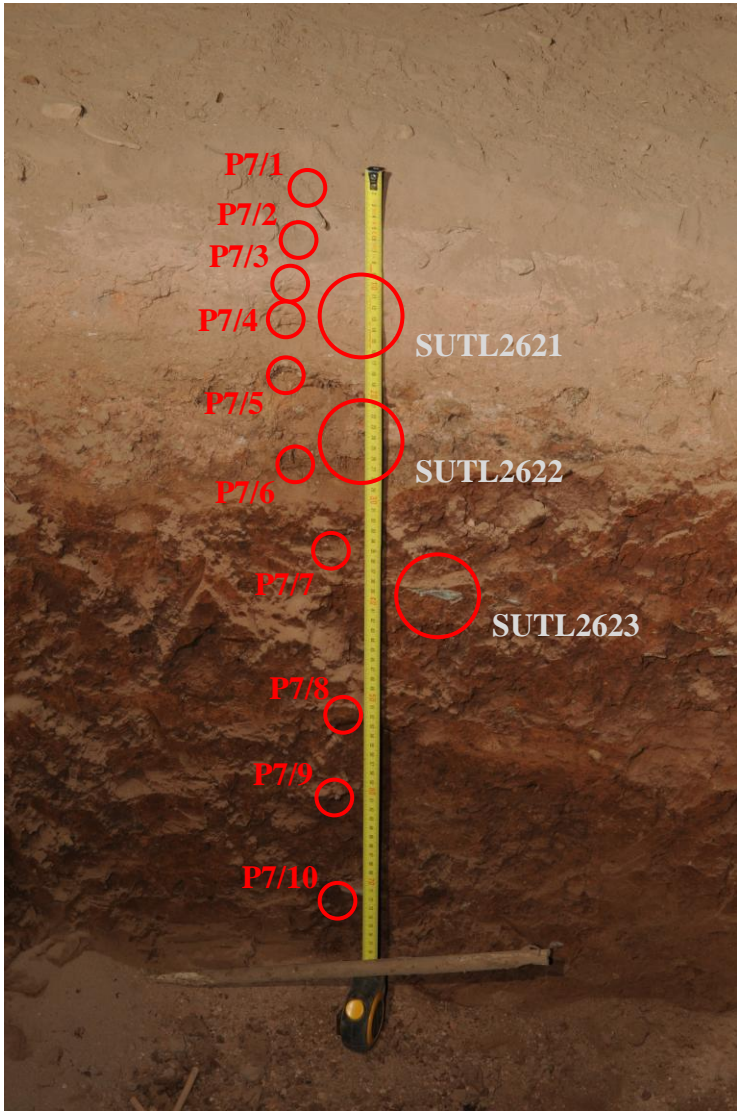


Figure 2-8: Profile 7, Test Pit 3, Kiptogot Cave
The positions of the field profiling samples are shown

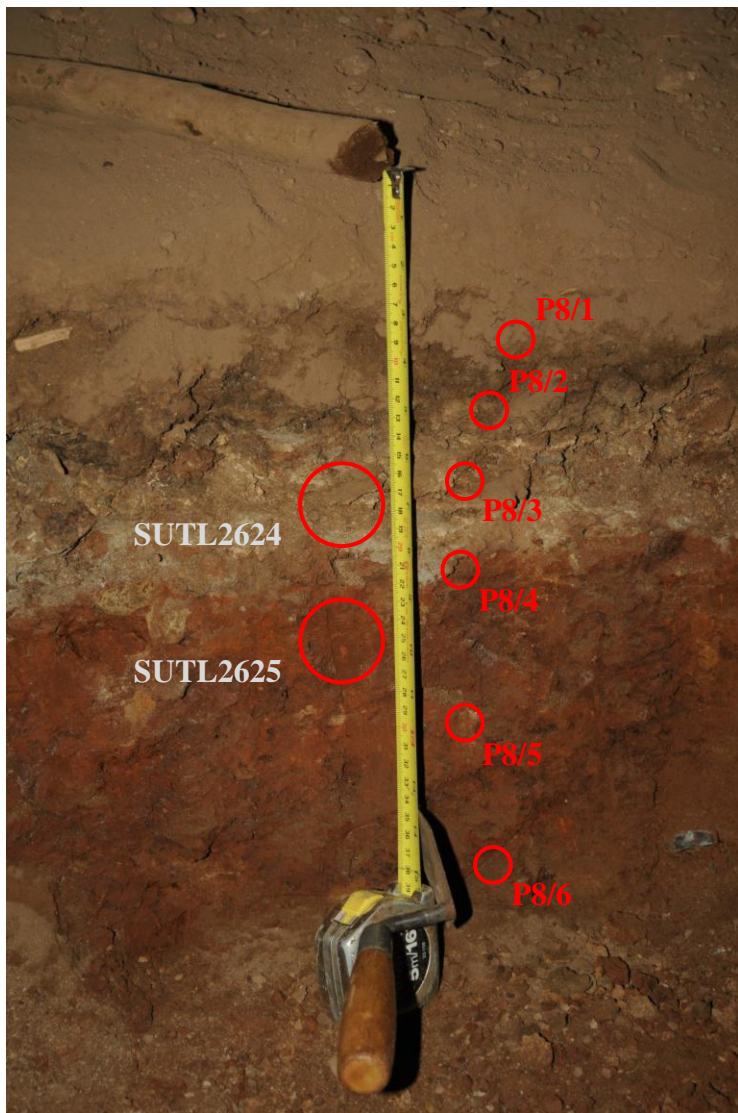
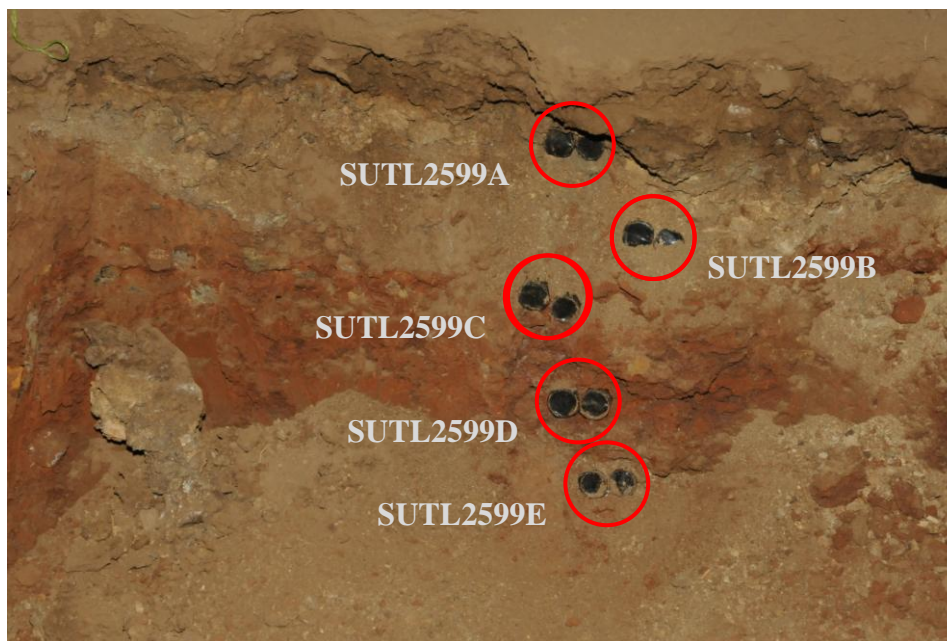


Figure 2-9: Profile 8, Test Pit 2, Kiptogot Cave
The positions of the field profiling samples are shown



3. Field Measurements

3.1. Dose rate measurements and determinations

Field Gamma Spectrometry (FGS) measurements were made using a Health Physics Instruments Rainbow MCA with a 2”x 2” NaI probe. Prior to fieldwork, measurements were made using this system on the doped concrete reference pads at SUERC in order to provide cross-reference to dose-rate conversion factors established by Sanderson in 1986, based on comparisons with TL dosimetry in doped blocks then at the Oxford and Risø luminescence laboratories. The spectra were calibrated to the 1457 keV peak from ⁴⁰K, then dose rates were determined from integral counts >450 keV, >1350 keV, and the energy integral (sum of counts times energy) across all the recorded spectrum. Using this approach yielded dose rates from the pads that were within errors of expected values.

Field spectra were each measured for 300s in holes cut around the luminescence sampling positions using a towel, and calibrated to the 1461 keV peak from ⁴⁰K before calculation of dose rates. Table 3-1 shows the mean gamma dose rates recorded in-situ for the dating samples. The mean gamma dose rate for all contexts, irrespective of cave, was 1.27 ± 0.04 mGy a⁻¹. In situ gamma dose rates are on average lower at Chepnyalil Cave (1.23 ± 0.03 mGy a⁻¹; n = 10) than at Kiptogot Cave (1.41 ± 0.12 mGy a⁻¹; n = 3)

Sample Ref	Context	Gamma Dose Rate / mGy a ⁻¹
<i>Chepnyalil Cave</i>		
SUTL2439	Profile 1, OSL1	1.25 ± 0.11
SUTL2440	Profile 1, OSL2	1.19 ± 0.10
SUTL2612	Profile 2, OSL1	1.16 ± 0.61
SUTL2613	Profile 2, OSL2	1.24 ± 0.60
SUTL2614	Profile 2, OSL3	1.20 ± 0.11
SUTL2615	Profile 2, OSL4	1.23 ± 0.11
-	Profile 2, infront	1.27 ± 0.11
-	Bedrock	0.62 ± 0.06
-	Bedrock	0.79 ± 0.07
SUTL2616	Profile 5, OSL1	1.07 ± 0.10
SUTL2617	Profile 5, OSL2	1.30 ± 0.11
SUTL2618	Profile 5, OSL3	1.39 ± 0.11
<i>Kiptogot Cave</i>		
SUTL2624	Profile 8, OSL1	1.25 ± 0.11
SUTL2625	Profile 8, OSL2	1.34 ± 0.12
SUTL2619	Profile 7, OSL1	1.64 ± 0.14

Table 3-1: In situ gamma dose rates measurements made using a Health Physics Instruments Rainbow MCA with a 2”x 2” NaI probe

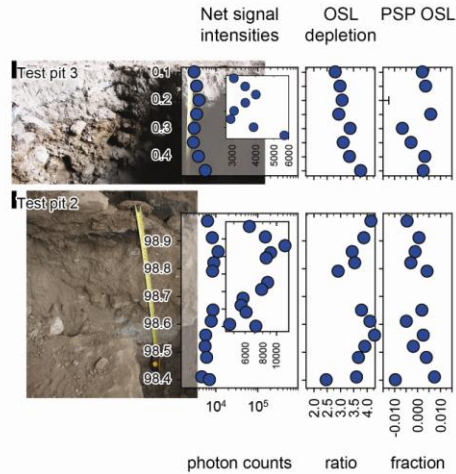
3.2. Field luminescence measurements

Field profiling measurements were made using a SUERC portable OSL reader, equipped with blue LEDs emitting around 470 nm, red LEDs emitting around 880 nm and UG11 detection filters. The blue diodes are outfitted with CG420 long pass filters,

whereas the IR diode ports are outfitted with RG780 long pass filters. Both signals pass through UG11 filters and detection is attained by a 24-bit photon counter set for unidirectional counting (Sanderson and Murphy, 2010). Full details on the instrument are provided in Sanderson and Murphy (2010). Samples were presented as bulk sediment in 50mm plastic petri dishes (stored in transparent PU bags), and the natural luminescence signals were measured following an interleaved sequence of system dark count (background), infra-red stimulated luminescence and optically stimulated luminescence, similar to that described by Sanderson and Murphy (2010). All profiling samples were measured on location in the field.

IRSL and OSL net signal intensities, depletion indices, IRSL/OSL ratios, post-stimulation IRSL and OSL phosphorescence, and post-stimulation phosphorescence (PSP) fractions for IRSL and OSL and their ratios are plotted against depth in figures 3-1 and 3-2 (the data are tabulated in Appendix B). The interpretation of the intensities, their depletion indices and the IRSL/OSL ratio have been discussed in Sanderson and Murphy (2010). Where minerals and the sediments have common sensitivities and dose rates the IRSL and OSL intensities may act as age proxies for well bleached sedimentary units, in which case inversions or discontinuities would reflect changes in initial residuality or in depositional circumstances. If sensitivity, colour or mineralogical origins change through the section, then intensities might also reflect those changes. The depletion index, which represents the proportion of signal released in the first half of the stimulation cycle relative to the second half, is an indicator of sample transparency coupled to information about whether the samples contained an inherited or single cycle signal. Higher depletion indices would indicate better bleached material. The IRSL/OSL ratio is potentially sensitive to mineralogical input changes, potentially reflecting quartz/feldspar relative contents and hence the weathering history of the sediment. These proxies can be used in combination with sedimentological observations to provide an initial interpretation of the luminescence stratigraphy.

Chepnyalil Cave
main cave



Chepnyalil Cave, Leopards Cave

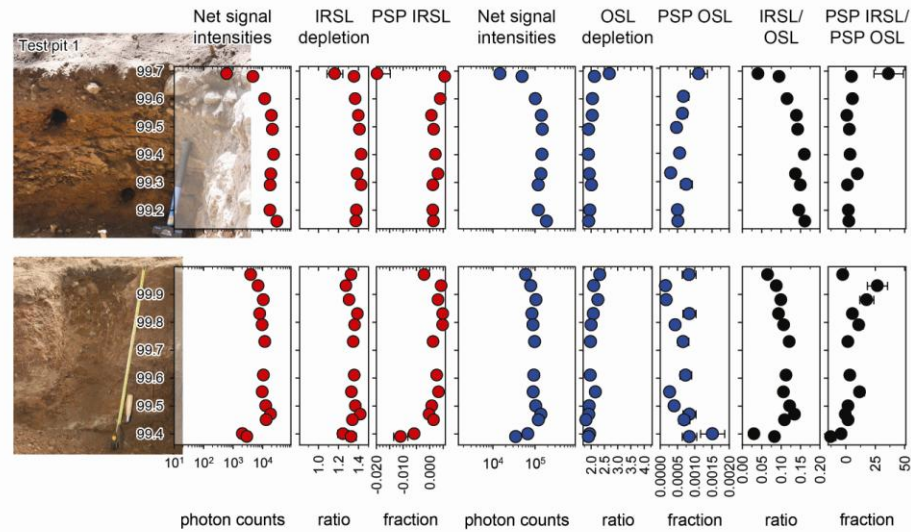
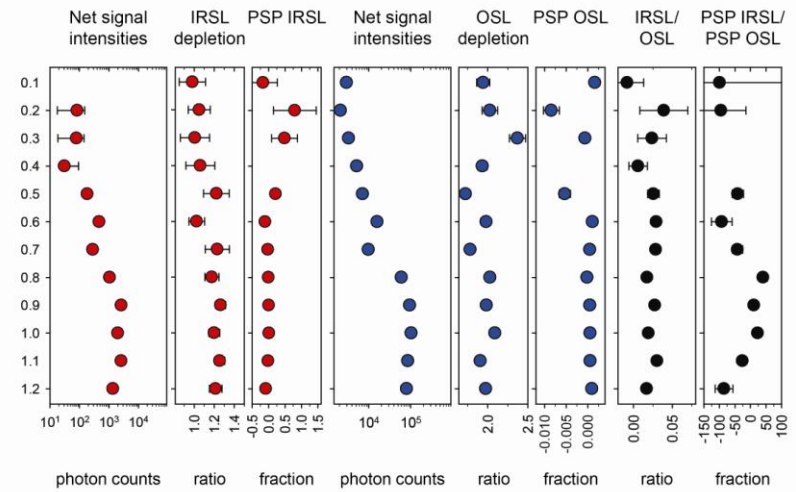


Figure 3-1: Field profiles from Chepnyalil Cave. The profiles on the left are from the main cave; the lower profiles encompass strata which has been previously dated to 15-20ka (J. Spencer, pers com.); the upper profiles encompass strata which has been previously dated to the 15th century (see table 1-1). The profile on the right is from the lower cave at Chepnyalil, the Leopards Cave.

Kiptogot Cave
main cave

Net signal
intensities OSL
depletion OSL
PSP

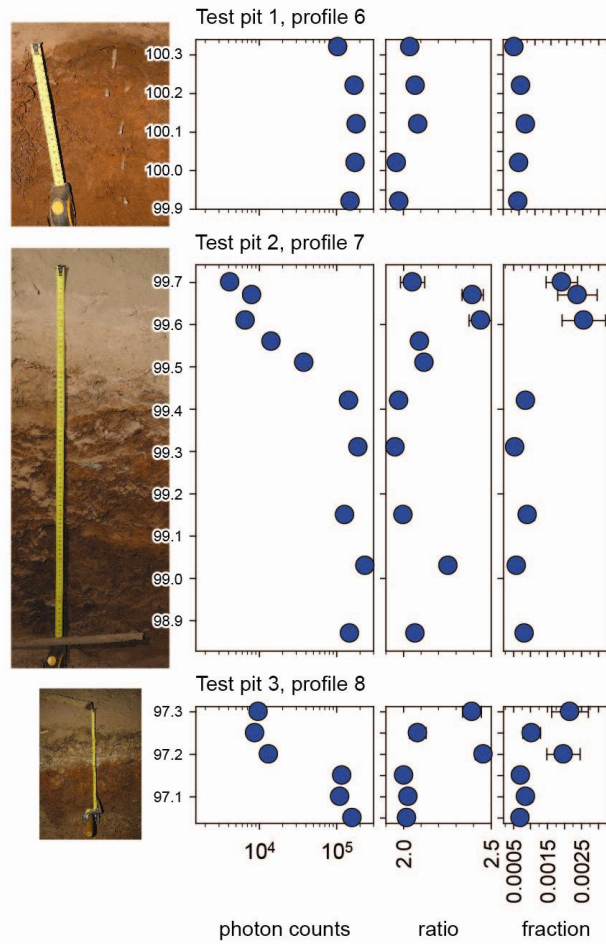


Figure 3-2: Field profiles from Kiptogot Cave.

The remaining two sediment stratigraphies sampled in the main Chepnyalil Cave enclose archaeological layers associated with a more recent occupation of the cave (on the basis of a radiocarbon age of 480 ± 30 yrs BP, cal AD 1410 to 1450, pottery finds, and stone typology). It is notable then, that the range in signal intensities obtained from sediment within both profiles are two orders of magnitude lower than those observed in profiles 1 and 2, ranging between $7 - 3 \times 10^3$ photon counts. In the first of the studied profiles, the bulk sediment shows an overall progression in luminescence signals with depth (P3/1 - P3/7), which is consistent with a normal age-depth progression. Interestingly, there is a spike in IRSL and OSL signal intensities, as the profile steps across the heated horizons (P3/1 - P3/4), including burnt earth and ash. It is possible that heating in historical time has sensitised the luminescence dosimeters within these horizons; given this maxima in signal intensity, it would be an easy matter to map out and correlate profiles on the basis of these heated materials. In the second profile, there is a slightly larger spread in IRSL and OSL signal intensities, suggesting that the stratigraphy in this profile is more complex, with variable bleaching at deposition. Notwithstanding this, the range in signal intensities is still informative, being a magnitude of 2 larger than those observed in profile 3. This is consistent with the available chronological data, which suggests that the sediment in this section is likely to be older (3rd - 4th centuries AD).

Therefore, it is recognised that a number of lithological/stratigraphic units can be distinguished on the basis of their luminescence characteristics (in approximate stratigraphic order):

- a compacted, red-brown clayey loam (designated unit A), which encloses the main artefact bearing horizons (*preserved at depth, c. 10 cm beneath the present cave floor in profiles 1 and 2*): characterised by consistently large IRSL and OSL net signal intensities (10^4 and 10^5 photon counts, respectively), and moderate depletion ratios (ratios of c. 1.3-1.4 and 2, respectively). Throughout this unit, signal intensities increase slightly with depth, consistent with a normal age-depth progression. This unit encompasses strata that has been previously dated by a conventional quartz SAR OSL approach to 15-23 ka (Table 1-1).
- poorly consolidated, red-brown to grey loams, passing upwards into brown loamy soils (unit B) (*preserved at the surface in profiles 1 and 2; and at depth, c. 45 to 100 cm in profiles 3 and 4*): characterised by moderate IRSL and OSL net signal intensities (10^2 and 10^3 photon counts, respectively), moderate IRSL depletion ratios (a ratio of c. 1. 3), and high OSL depletion ratios. Luminescence proxy characteristics remain relatively similar through this unit, implying that this material accumulated very rapidly. This unit constrains strata that has been previously been dated to c. 15th century AD (Table 1-1)
- heated materials (unit C), including reddened earth and ash layers (*preserved from c. 45-35 cm to the surface in profiles 3 and 4*): characterised by maxima in signal intensities, above the background levels, and high depletion ratios.
- modern materials (unit D), characterised by the lowest signal intensities, observed in the profiles.

Following the initial luminescence investigations in the main Chepnylil cave, and the characterisation of the luminescence properties of sediment of known age, it is possible to place the sediment profiled in the lower cave into a relative stratigraphic sequence. It is notable that the basal samples from the Leopard Cave profile (between a depth of 80 and 120 cm; P5/8 to P5/12) have similar IRSL and OSL signal intensities to those observed in the lower parts of profiles 1 and 2 (luminescence unit A). Further up the profile (P5/7 to P5/5), the OSL signal intensities are comparable to those observed in the basal layer of profile 4 (9.7×10^3 and 7×10^3 photon counts, respectively), with similar OSL depletion ratios (c. 2). This middle unit contains strata previously dated to the 3rd to 4th century AD, on the basis that the sediment encloses a charcoal fragment dated to 1680 ± 30 yrs BP. As such, a further luminescence unit is defined, unit Bi, characterised by OSL net signal intensities on the order of 9.7×10^3 photon counts. At the top of the profile (P5/4 to P5/1) the range in observed signal intensities are comparable to that observed in profile 3, suggesting that these units may be time equivalent.

It is also tempting to draw correlations between the sediment-OSL stratigraphies at Chepnylil with those at Kiptogot. Interestingly, the Kiptogot profiles are characterised by a similar luminescence ‘sequence’, with distinct luminescence properties: (i) the strata resting on bedrock, and preserved at variable thicknesses (15 - 50 cm), returns large OSL net signal intensities, and moderate depletion ratios, comparable to unit A above; (ii) a variably preserved, discontinuous, unit of poorly consolidated, red-brown to grey loams, uncomfortably resting on the lower unit, is characterised by moderate net signal intensities comparable to units B/Bi and C); and (iii) the upper horizons, passing into the modern topsoil, characterised by low net signal intensities.

In summary, the use of the portable reader facilitated the rapid analysis of 76 sediment samples, which coupled with the existing chronological constraints (Table 1-1), allows discrete parts of each profile to be placed within a relative chronological sequence. As such, even withstanding the numerous variable which influence the luminescence proxy-depth plots, it is possible to correlate (in realtime) different lithological and stratigraphic units, both temporally and spatially between test-pits (and between sites). Having identified parts of the cores with similar and dissimilar luminescence characteristics as outlined above, sections were identified for further dating analysis. First luminescence profiling was used from selected samples to assess sensitivity and obtain the first evidence which could indicate the magnitude of the ages implied, and also provide first assessment of whether or not the sediments chosen for dating might be well bleached. These results confirm that the materials chosen are broadly consistent with several temporal units, in line with the multi-phase occupation of both Chepnylil and Kiptogot Cave in the LSA, and Medieval periods. The quantitative dating analyses follow from this.

4. Calibrated laboratory luminescence screening measurements

4.1. Methodology

All sample handling and preparation was conducted under safelight conditions in the SUERC luminescence dating laboratories. The profiling samples were wet sieved to extract the 90-250 μm fractions, which were then treated with 1M HCl for 10 minutes. The samples were split into two fractions, one for polymineral analysis and one for quartz analysis. The quartz subsample was treated with 40% HF for 40 minutes, to dissolve the less chemically resistant minerals and to etch the outer part of the grains. The HF etched material was then treated with 1 M HCl for 10 minutes to dissolve any precipitated fluorides. The grains were presented for measurement on 10 mm in diameter stainless steel discs.

Luminescence sensitivities (Photon Counts per Gy) and stored doses (Gy) were evaluated from paired aliquots of the HF-etched quartz and polymineral fractions, using Risø DA-15 automatic readers (following procedures established in Burbidge et al., 2007; Sanderson et al., 2001; Sanderson et al., 2003). The readout cycles comprised a natural readout, followed by readout cycles for a nominal 1Gy test dose, a 5Gy regenerative dose, and a further 1Gy test dose. For the quartz samples, a 240°C preheat was used with 60s OSL measurements using the blue LEDs. For the polymineral samples, a 260°C preheat was followed by 60s OSL measurements using the IR LEDs at 50°C, the IR LEDs at 225°C (the post-IR IRSL signal), the blue LEDs at 125°C, and a TL measurement to 500°C.

4.2. Results

The data are tabulated below, and presented graphically in figures 4-1 to 4-3, for the three profiles respectively. Laboratory profiling provides preliminary assessments of stored doses and luminescence sensitivities in sediment collected from Chepnyalil Cave (profile 2, 3 samples enclosing the dating samples) and Kiptogot Cave (profiles 7 and 8, 6 samples each enclosing the dating samples). The OSL stored dose results reproduce the apparent maxima/trends in the luminescence proxy data set (with the exception of samples P7/8 and P7/10, see below). Moreover, the data support the correlations suggested by the field profiling dataset: for example that strata beneath 10 cm in profiles 1 and 2, Chepnyalil Cave (quartz OSL stored dose > 25 Gy, with good reproducibility between aliquots), correlate broadly with the strata beneath 20 cm and 5 cm in profiles 7 and 8, respectively, Kiptogot Cave (quartz OSL stored dose > 20 - 25 Gy, with good reproducibility between aliquots).

SUTL no.	Equivalent to	HOD	Stored dose / Gy		Sensitivity / Photon counts Gy ⁻¹		Stored dose / Gy	Sensitivity / Photon counts Gy ⁻¹
			aliquot 1	aliquot 2	aliquot 1	aliquot 2		
Chepnyalil Cave, Test Pit 1								
2597/A	P2/2	99.90	17.1 ± 0.2	14.4 ± 0.2	14000 ± 60	7800 ± 40	15.7 ± 1.3 (0.3)	10900 ± 3100 (70)
2597/B	P2/5	99.75	25.2 ± 0.3	28.2 ± 0.5	13890 ± 60	5290 ± 40	26.7 ± 1.5 (0.5)	9590 ± 4300 (70)
2597/C	P2/7	99.68	27.4 ± 0.4	25.6 ± 0.3	5540 ± 40	10990 ± 50	26.5 ± 0.9 (0.5)	8260 ± 2730 (70)
Kiptogot Cave, Test Pit 2								
2598/A	P7/1	99.70	2.1 ± 0.1	2.5 ± 0.1	8810 ± 50	10370 ± 50	2.3 ± 0.2 (0)	9590 ± 780 (70)
2598/B	P7/2	99.67	12.0 ± 0.1	11.8 ± 0.1	35450 ± 90	61460 ± 120	11.9 ± 0.1 (0.1)	48460 ± 13010 (150)
2598/C	P7/5	99.51	17.3 ± 0.1	16.4 ± 0.1	36080 ± 90	104060 ± 160	16.9 ± 0.4 (0.1)	70070 ± 33990 (190)
2598/D	P7/8	99.15	2.0 ± 0.1	1.8 ± 0.1	7500 ± 40	10400 ± 50	1.9 ± 0.1 (0)	8950 ± 1450 (70)
2598/E	P7/10	98.87	4.3 ± 0.0	10.1 ± 0.1	23750 ± 80	24370 ± 80	7.2 ± 2.9 (0.1)	24060 ± 310 (110)
2598/F	-	98.57	18 ± 0.2	18.2 ± 0.1	15550 ± 60	73690 ± 140	18.1 ± 0.1 (0.2)	44620 ± 29070 (150)
Kiptogot Cave, Test Pit 3								
2599/A	P8/2	97.25	5.5 ± 0.2	2.0 ± 0.1	1560 ± 20	5470 ± 40	3.8 ± 1.8 (0.2)	3520 ± 1960 (40)
2599/B	P8/3	97.20	18.5 ± 0.1	22.3 ± 0.1	31560 ± 90	62240 ± 130	20.4 ± 1.9 (0.2)	46900 ± 15340 (150)
2599/C	P8/4	97.10	15.1 ± 0.8	-	720 ± 20	-	8.5 ± 6.6 (0.9)	1620 ± 900 (30)
2599/D	P8/5	97.00	16.0 ± 0.5	28.3 ± 0.1	1880 ± 20	64550 ± 120	22.1 ± 6.2 (0.5)	33210 ± 31330 (130)
2599/E	P8/6	96.90	27.9 ± 0.1	-	67130 ± 130	-	-	-

Table 4-1: Quartz (HF-etched) stored dose and sensitivity estimates obtained using a simplified two-step OSL SAR procedure

SUTL no.	Equivalent to	HOD	Stored dose / Gy		Sensitivity / Photon cts Gy ⁻¹		Stored dose / Gy	Sensitivity / Photon counts Gy ⁻¹
			aliquot 1	aliquot 2	1	2		
Chepnyalil Cave, Test Pit 1								
2597/A	P2/2	99.90						
2597/B	P2/5	99.75	276.5 ± 6.3	199.6 ± 7	263 ± 2	126 ± 2	238 ± 38.5 (9.5)	190 ± 70 (3)
2597/C	P2/7	99.68	448.1 ± 8.6	255.7 ± 7.1	352 ± 3	185 ± 2	351.9 ± 96.2 (11.1)	270 ± 80 (3)
Kiptogot Cave, Test Pit 2								
2598/A	P7/1	99.70	33 ± 0.9	15.5 ± 0.5	278 ± 2	303 ± 3	24.2 ± 8.8 (1)	290 ± 10 (4)
2598/B	P7/2	99.65	20.1 ± 0.9	33.9 ± 2.3	132 ± 2	57 ± 1	27 ± 6.9 (2.4)	90 ± 40 (2)
2598/C	P7/5	99.48	130.3 ± 18.2	163.3 ± 6	22 ± 1	118 ± 2	146.8 ± 16.5 (19.1)	70 ± 50 (2)
2598/D	P7/8	99.15	98.2 ± 4.2	93.8 ± 1.7	92 ± 2	425 ± 3	96 ± 2.2 (4.5)	260 ± 170 (3)
2598/E	P7/10	98.55	256.3 ± 10	302.1 ± 8.2	112 ± 2	212 ± 2	279.2 ± 22.9 (12.9)	160 ± 50 (3)
2598/F	-	97.57	282.4 ± 3.9	291.4 ± 4.1	700 ± 4	689 ± 4	286.9 ± 4.5 (5.7)	690 ± 10 (6)
Kiptogot Cave, Test Pit 3								
2599/A	P8/2	97.25	88.9 ± 3.6	27.7 ± 0.5	108 ± 2	452 ± 3	58.3 ± 30.6 (3.6)	280 ± 170 (4)
2599/B	P8/3	97.20	90.2 ± 7.8	39.2 ± 1.4	37 ± 1	133 ± 2	64.7 ± 25.5 (8)	80 ± 50 (2)
2599/C	P8/4	97.10	286.9 ± 4.1	308.1 ± 3.5	661 ± 4	996 ± 5	297.5 ± 10.6 (5.3)	830 ± 170 (6)
2599/D	P8/5	97.00	425.4 ± 6.7	351.6 ± 11.2	524 ± 3	159 ± 2	388.5 ± 36.9 (13)	340 ± 180 (4)
2599/E	P8/6	96.90	223.8 ± 15	-	55 ± 1	-	-	-

Table 4-2: Polymineal stored dose and sensitivity estimates obtained using a simplified two-step post-IRSL OSL SAR procedure

Chepnaylil Cave, Profile 2. Laboratory profiling samples were collected from strata enclosing the full dating samples - SUTL 2613, 2614 and 2615. Quartz OSL stored dose estimates are observed to increase with depth, from c. 15 Gy to 25 Gy, through the unit. Interestingly, the paired quartz OSL stored dose estimates obtained for the lower units in this profile are similar; suggesting that this material may have been well bleached at deposition.

Kiptogot Cave, Profile 8. The associated luminescence proxy-depth profile for the sediment stratigraphy preserved in test-pit 4, suggests a temporal division between the lower and upper parts of the sequence. Laboratory profiling confirms this temporal division: quartz stored dose estimates range between c. 2 and 5 Gy in the upper layers, and between 15 and 25 Gy in the lower layers. As at Chepnaylil, the quartz OSL stored dose estimates increase slightly with depth, implying a normal age depth progression, and a fast accumulation rate.

5. Quartz SAR/alkali feldspar SARA measurements

5.1. Sample preparation

All sample handling and preparation was conducted under safelight conditions in the SUERC luminescence dating laboratories.

5.1.1. Water contents

Bulk samples were weighed, saturated with water and re-weighed. Following oven drying at 50 °C to constant weight, the actual and saturated water contents were determined as fractions of dry weight. These data were used, together with information on field conditions to determine water contents and an associated water content uncertainty for use in dose rate determination.

5.1.2. HRGS and TSBC Sample Preparation

Bulk quantities of material, weighing c. 50g, were removed from each full dating sample for environmental dose rate determinations. This material was placed in an oven to dry to constant weight. Approximately 50g quantities of dried material from each sample were weighed into HDPE pots for a high-resolution gamma spectrometry (HRGS) measurement. Each pot was sealed with epoxy resin and left for 3 weeks prior to measurement to allow equilibration of ²²²Rn daughters. A further 20 g of the dried material was used in thick source beta counting (TSBC; Sanderson, 1988b).

5.1.3. Quartz/feldspar Sample Preparation

Approximately 20g of material was removed for each tube and processed for luminescence measurements, to separate sand-sized quartz and feldspar grains. The sample was wet sieved to obtain the 90-150 and 150-250 µm fractions. The 150-250 µm sub-sample was treated with 1 M hydrochloric acid (HCl) for 10 minutes, 15% hydrofluoric acid (HF) for 15 minutes, and 1 M HCl for a further 10 minutes. This

etched material was then centrifuged in sodium polytungstate solutions of ~2.51, 2.58, 2.62, and 2.74 gcm⁻³, to obtain concentrates of potassium-rich feldspars (2.51-2.58 gcm⁻³), sodium feldspars (2.58-2.62 gcm⁻³) and quartz plus plagioclase (2.62-2.74 gcm⁻³). The selected quartz fraction was then subjected to further HF and HCl washes (40% HF for 40mins, followed by 1M HCl for 10 mins). All materials were dried at 50°C and transferred to Eppendorf tubes. The 15% HF-etched, 2.51-2.58 gcm⁻³ polymineral, and 40%HF-etched, 2.62-2.74 gcm⁻³ ‘quartz’ fractions were dispensed to 10mm stainless steel discs for measurement. 16 aliquots were produced for all samples.

5.2. Measurements and determinations

5.2.1. Dose rate determinations

Dose rates were measured in the laboratory using HRGS and TSBC. HRGS dose rate determinations were made for all samples, coupled with TSBC dose rate determinations on samples SUTL2612-13, 2620 and 2626-27.

HRGS measurements were performed using a 50% relative efficiency “n” type hyper-pure Ge detector (EG&G Ortec Gamma-X) operated in a low background lead shield with a copper liner. Gamma ray spectra were recorded over the 30 keV to 3 MeV range from each sample, interleaved with background measurements and measurements from SUERC Shap Granite standard in the same geometries. Samples were counted for 160ks. The spectra were analysed to determine count rates from the major line emissions from ⁴⁰K (1461 keV), and from selected nuclides in the U decay series (²³⁴Th, ²²⁶Ra + ²³⁵U, ²¹⁴Pb, ²¹⁴Bi and ²¹⁰Pb) and the Th decay series (²²⁸Ac, ²¹²Pb, ²⁰⁸Tl) and their statistical counting uncertainties. Net rates and activity concentrations for each of these nuclides were determined relative to Shap Granite by weighted combination of the individual lines for each nuclide. The internal consistency of nuclide specific estimates for U and Th decay series nuclides was assessed relative to measurement precision, and weighted combinations used to estimate mean activity concentrations (Bq kg⁻¹) and elemental concentrations (% K and ppm U, Th) for the parent activity. These data were used to determine infinite matrix dose rates for alpha, beta and gamma radiation.

Beta dose rates were also measured directly using the SUERC TSBC system (Sanderson, 1988b). Sample count rates were determined with six replicate 600 s counts for each sample, bracketed by background measurements and sensitivity determinations using the Shap Granite secondary reference material. Infinite-matrix dose rates were calculated by scaling the net count rates of samples and reference material to the working beta dose rate of the Shap Granite (6.25 ± 0.03 mGy a⁻¹). The estimated errors combine counting statistics, observed variance and the uncertainty on the reference value.

The dose rate measurements were used in combination with the assumed burial water contents, to determine the overall effective dose rates for age estimation. Cosmic dose rates were evaluated by combining latitude and altitude specific dose rates (0.18 ± 0.01 mGy a⁻¹) for the site with corrections for estimated depth of overburden using the method of Prescott and Hutton (1994).

5.2.2. Exploratory quartz / feldspar SAR determinations

All measurements were conducted using a Risø DA-15 automatic reader equipped with a $^{90}\text{Sr}/^{90}\text{Y}$ β -source for irradiation, blue LEDs emitting around 470 nm and infrared (laser) diodes emitting around 830 nm for optical stimulation, and a U340 detection filter pack to detect in the region 270-380 nm, while cutting out stimulating light (Bøtter-Jensen et al., 2000). For each sample, equivalent dose determinations were made on sets of 4 aliquots per sample (2 aliquots of quartz, 2 aliquots of K feldspar), using a single aliquot regeneration (SAR) sequence (cf Murray and Wintle, 2000). This sequence is described in full below.

The readout cycles comprised a natural readout, followed a nominal 1.6 Gy test dose, and regenerative doses of 0.8, 2, 4, 8, 40, 80, 160 and 2 Gy, followed by the 1.6 Gy test dose. For the quartz samples, a 240°C preheat was used with 60s OSL measurements using the blue LEDs. For the polymineral samples, a 240°C preheat was followed by 60s OSL measurements using the IR LEDs at 50°C, the IR LEDs at 200°C (the post-IR IRSL signal), 250°C and 300°C (the post-IR IRSL signals at elevated temperatures).

5.2.3. Exploratory feldspar SARA luminescence measurements

All measurements were performed on the same equipment described above. Equivalent dose determinations were made using a single aliquot regenerative additive dose protocol combining the SARA approach (Mejdahl and Bøtter-Jensen, 1994, 1997) with longer overnight preheating as discussed by Alexander (2007) to mitigate short term fading. In the original SARA method groups of aliquots were formed with added doses, and a linear dose estimate made for each aliquot by scaling luminescence signals between the first (natural plus added dose) and a regenerated signal. Dose estimates are formed by regression of the added dose response curves to zero signal. In the modification suggested by Alexander, long overnight preheating is introduced before the first readout, so that both natural and added doses are stabilised in the manner suggested by Sanderson (1988a). Automated readout with regenerative dose pre-heated in the instrument completes the sequence. This was implemented here with sets of 15 aliquots, sub-divided into 5 groups of 3 aliquots (natural, natural + 2.2 Gy, natural + 4.3 Gy, natural + 8.6 Gy, natural + 43.1 Gy). Irradiations were performed using an automated Elsec irradiator equipped with a 1.85Gbpq ^{90}Sr source (dose rate 1.76 Gy/min at time of the experiment). The experimental conditions were as follows: the IRSL from the natural and natural + β dose aliquots was recorded after a 16 hr preheat at 120°C; the test dose response was recorded after a 30 s preheat at 200°C; and IRSL measurements at 50°C were conducted over 60 s, with backgrounds recorded before and after stimulation.

5.2.4. Quartz OSL SAR measurements

Full quartz SAR OSL determinations were made on the same Risø DA-15 automatic readers as described above. Equivalent dose determinations were made using a single aliquot OSL SAR method on sets of 12-16 aliquots. According to this procedure, the OSL signal level from an individual disc is calibrated to provide an absorbed dose estimate (the equivalent dose) using an interpolated dose-response

curve, constructed by regenerating OSL signals by beta irradiation in the laboratory. Sensitivity changes which may occur as a result of readout, irradiation and preheating (to remove unstable radiation-induced signals) are monitored using small test doses after each regenerative dose. Each measurement is standardised to the test dose response determined immediately after its readout, to compensate for observed changes in sensitivity during the laboratory measurement sequence. For the purposes of interpolation, the regenerative doses are chosen to encompass the likely value of the equivalent (natural) dose (determined in the initial laboratory characterisation study, see section 4). A repeat dose point is included to check the ability of the SAR procedure to correct for laboratory-induced sensitivity changes (the ‘recycling test’), a zero dose point is included late in the sequence to check for thermally induced charge transfer during the irradiation and preheating cycle (the ‘zero cycle’), and an IR response check is included to assess the magnitude of non-quartz signals. To assess the dependence of equivalent dose on preheat, four different preheat temperatures were investigated (200, 220, 240 and 260°C).

5.3. Results

5.3.1. Dose rates

HRGS results are shown in Table 5-1, both as activity concentrations (i.e. disintegrations per second per kilogram) and as equivalent parent element concentrations (in % and ppm), based in the case of U and Th on combining nuclide specific data assuming decay series equilibrium.

SUTL no.	Activity Concentration ^a / Bq kg ⁻¹			Equivalent Concentration ^b		
	K	U	Th	K / %	U / ppm	Th / ppm
Chepnyalil Cave						
2612	810 ± 21	46 ± 4	63 ± 2	2.62 ± 0.07	3.71 ± 0.29	15.49 ± 0.49
2613	673 ± 18	51 ± 4	71 ± 2	2.18 ± 0.06	4.16 ± 0.29	17.53 ± 0.48
2613B	666 ± 18	54 ± 5	54 ± 2	2.15 ± 0.06	4.35 ± 0.39	13.27 ± 0.42
2614	638 ± 19	48 ± 4	69 ± 2	2.06 ± 0.06	3.86 ± 0.31	16.99 ± 0.53
2615	594 ± 17	49 ± 3	76 ± 2	1.92 ± 0.06	3.97 ± 0.26	18.63 ± 0.47
2615B	598 ± 17	52 ± 5	55 ± 2	1.93 ± 0.05	4.24 ± 0.37	13.68 ± 0.42
2616	586 ± 17	34 ± 2	48 ± 2	1.89 ± 0.05	2.78 ± 0.19	11.88 ± 0.38
2617	466 ± 17	31 ± 3	43 ± 2	1.51 ± 0.06	2.53 ± 0.21	10.59 ± 0.43
2618	336 ± 16	66 ± 5	90 ± 2	1.09 ± 0.05	5.37 ± 0.40	22.26 ± 0.59
Leopards Cave (Lower Chepnyalil Cave)						
2619	603 ± 30	27 ± 6	46 ± 5	1.95 ± 0.10	2.17 ± 0.45	11.46 ± 1.23
2620	370 ± 15	33 ± 3	54 ± 2	1.19 ± 0.05	2.67 ± 0.22	13.19 ± 0.44
Kiptogot Cave						
2621	1489 ± 25	37 ± 2	47 ± 2	4.82 ± 0.08	2.99 ± 0.20	11.64 ± 0.39
2622	1801 ± 27	45 ± 3	57 ± 2	5.82 ± 0.09	3.61 ± 0.23	14.07 ± 0.40
2623	622 ± 19	39 ± 3	70 ± 2	2.01 ± 0.06	3.12 ± 0.26	17.21 ± 0.52
2624	889 ± 18	29 ± 2	35 ± 1	2.88 ± 0.06	2.37 ± 0.15	8.60 ± 0.31
2624B	850 ± 19	23 ± 2	49 ± 2	2.75 ± 0.06	1.86 ± 0.19	12.16 ± 0.38
2625	560 ± 17	38 ± 3	62 ± 2	1.81 ± 0.05	3.05 ± 0.23	15.39 ± 0.44
2626	846 ± 19	21 ± 2	31 ± 1	2.74 ± 0.06	1.67 ± 0.13	7.61 ± 0.33
2627	515 ± 17	25 ± 2	44 ± 2	1.66 ± 0.05	1.99 ± 0.18	10.77 ± 0.40
Chepnyalil Cave - collected in 2012						

2439	801 ± 21	55 ± 3	74 ± 2	2.59 ± 0.07	4.48 ± 0.28	18.15 ± 0.52
2440	875 ± 21	71 ± 5	87 ± 2	2.83 ± 0.07	5.72 ± 0.38	21.44 ± 0.6

Table 5-1: Activity and equivalent concentrations of K, U and Th determined by HRGS

^aShap granite reference, working values determined by David Sanderson in 1986, based on HRGS relative to CANMET and NBL standards.

^bActivity and equivalent concentrations for U, Th and K determined by HRGS (Conversion factors based on NEA (2000) decay constants): 40K: 309.3 Bq kg⁻¹ %K⁻¹, 238U: 12.35 Bq kg⁻¹ ppmU⁻¹, 232Th: 4.057 Bq kg⁻¹ ppm Th⁻¹.

Infinite matrix alpha, beta and gamma dose rates from HRGS are listed for all samples in Table 4-2, together with infinite matrix beta dose rates from TSBC, and in situ gamma dose rates from FGS (section 3.1). In general, there is a good agreement between TSBC and HRGS beta dose rate estimates, and FGS and HRGS gamma dose rate estimates (ratios, 1.1 ± 0.3 and 0.9 ± 0.3, respectively).

The water content measurements with assumed values for the average water content during burial are given in Table 4-3. The table also lists the gamma dose rate from the HRGS after application of a water content correction. Effective dose rates to the HF etched 200 µm quartz grains are given for the gamma dose rate and beta dose rate (the mean of the TSBC and HRGS data, accounting for water content and grain size). The mean effective dose rate is 3.39 ± 0.26 mGy a⁻¹, varying slightly between sites, 3.53 ± 0.33 mGy a⁻¹ at Chepnyalil and 3.00 ± 0.15 mGy a⁻¹ at Kiptogot.

SUTL no.	HRGS, dry ^a / mGy a ⁻¹			TSBC, dry / mGy a ⁻¹	FGS, wet / mGy a ⁻¹
	Alpha	Beta	Gamma		
Chepnyalil Cave					
2612	21.76 ± 0.89	3.16 ± 0.07	1.85 ± 0.04	3.36 ± 0.10	1.16 ± 0.10
2613	24.50 ± 0.88	2.91 ± 0.07	1.90 ± 0.04	2.93 ± 0.09	1.24 ± 0.11
2614	23.29 ± 0.94	2.76 ± 0.07	1.81 ± 0.05	-	1.20 ± 0.11
2615	24.79 ± 0.81	2.71 ± 0.06	1.88 ± 0.04	-	1.23 ± 0.11
2616	16.50 ± 0.60	2.32 ± 0.05	1.39 ± 0.03	-	1.07 ± 0.10
2617	14.85 ± 0.67	1.92 ± 0.06	1.20 ± 0.04	-	1.30 ± 0.11
2618	31.38 ± 1.19	2.32 ± 0.07	2.02 ± 0.06	-	1.39 ± 0.11
Leopards Cave (Lower Chepnyalil Cave)					
2619	14.50 ± 1.55	2.26 ± 0.11	1.31 ± 0.09	-	1.64 ± 0.14
2620	17.18 ± 0.70	1.76 ± 0.05	1.27 ± 0.04	1.95 ± 0.07	-
Kiptogot Cave					
2621	16.92 ± 0.62	4.77 ± 0.07	2.10 ± 0.04	-	-
2622	20.44 ± 0.71	5.76 ± 0.08	2.54 ± 0.04	-	-
2623	21.39 ± 0.81	2.62 ± 0.06	1.73 ± 0.04	-	-
2624	12.95 ± 0.47	2.98 ± 0.05	1.41 ± 0.03	-	1.25 ± 0.11
2625	19.84 ± 0.71	2.39 ± 0.06	1.58 ± 0.03	-	1.34 ± 0.12
2626	10.25 ± 0.44	2.73 ± 0.06	1.58 ± 0.03	3.05 ± 0.09	-
2627	13.48 ± 0.57	1.98 ± 0.05	1.18 ± 0.03	2.34 ± 0.08	-
Chepnyalil Cave - collected in 2012					
2439	25.86 ± 0.87	3.32 ± 0.07	2.07 ± 0.04	3.43 ± 0.07	-
2440	31.74 ± 1.13	3.80 ± 0.08	2.44 ± 0.06	3.84 ± 0.08	-

Table 5-2: Infinite matrix dose rates determined by HRGS and TSBC.

^abased on dose rate conversion factors in Aikten (1983) and Sanderson (1987)

SUTL No.	Water Content / %			Effective Dose Rate / mGy a ⁻¹		
	Fractional	Saturated	Assumed	Beta ^a	Gamma	Total ^b
Chepnyalil Cave						
2612	9.4	24.2	13 ± 3	2.38 ± 0.13	1.35 ± 0.13	3.83 ± 0.19
2613	16.3	33.5	21 ± 5	2.06 ± 0.14	1.39 ± 0.16	3.55 ± 0.21
2614	17.2	32.6	21 ± 5	1.77 ± 0.11	1.24 ± 0.14	3.11 ± 0.18
2615	19.5	32.1	23 ± 6	1.86 ± 0.12	1.35 ± 0.15	3.31 ± 0.20
2616	22.9	40.1	27 ± 7	1.55 ± 0.10	1.10 ± 0.14	2.75 ± 0.17
2617	20.1	34.4	24 ± 6	1.32 ± 0.09	1.04 ± 0.14	2.46 ± 0.16
2618	27.1	32.1	28 ± 7	1.54 ± 0.12	1.46 ± 0.18	3.10 ± 0.21
Leopards Cave (Lower Chepnyalil Cave)						
2619	21.2	33.5	24 ± 6	1.58 ± 0.12	1.27 ± 0.18	2.95 ± 0.22
2620	24.7	31.4	26 ± 7	1.25 ± 0.10	0.98 ± 0.06	2.34 ± 0.12
Kiptogot Cave						
2621	10.5	16.9	12 ± 3	3.60 ± 0.15	1.77 ± 0.09	5.46 ± 0.18
2622	17.1	39.6	23 ± 6	4.03 ± 0.23	2.03 ± 0.11	6.16 ± 0.25
2623	19.9	35.2	24 ± 6	1.81 ± 0.11	1.37 ± 0.08	3.28 ± 0.14
2624	37.4	48.9	23 ± 6	2.06 ± 0.13	1.19 ± 0.14	3.35 ± 0.19
2625	24.2	37.6	28 ± 7	1.59 ± 0.11	1.27 ± 0.14	2.97 ± 0.18
2626	15.3	30.8	19 ± 5	2.09 ± 0.13	1.06 ± 0.07	3.25 ± 0.15
2627	24.7	36.4	28 ± 7	1.44 ± 0.11	0.91 ± 0.06	2.45 ± 0.13
Chepnyalil Cave - collected in 2012						
2439	22.4	29.8	22 ± 5	2.37 ± 0.14	1.67 ± 0.08	4.03 ± 0.14
2440	26.6	33.0	22 ± 5	2.67 ± 0.15	1.96 ± 0.10	4.63 ± 0.16

Table 5-3: Water contents, and effective beta and gamma dose rates following water correction.

^a Effective beta dose rate combining water content corrections with inverse grain size attenuation factors obtained by weighting the 200 µm attenuation factors of Mejdahl (1979) for K, U, and Th by the relative beta dose contributions for each source determined by Gamma Spectrometry.

5.3.2. Exploratory quartz / feldspar SAR screening measurements

Previous investigations (Kinnaird et al., 2012) have shown that to date the full range of sediments at Chepnyalil and Kiptogot it would be necessary to employ a range of luminescence procedures from conventional quartz SAR analyses to protocols which exploit deeper trap signals in both quartz and K feldspar. Therefore, it was necessary to subject all dating samples, to simplified SAR OSL and IRSL SAR-type procedures, to determine the most suitable protocol for each dating sample. The conventional quartz OSL signals from the Chepnyalil and Kiptogot Cave quartz saturates in the region of 75-80 Gy (composite dose response curves generated for each sample, based on a simplified SAR procedure on paired aliquots, are presented in Appendix C). This thereby limits the dating range to 19 - 20 ka, assuming an average total environmental dose of 3.4 ± 0.3 mGy a⁻¹.

In contrast, the IRSL at 50°C continues to grow linearly to doses up to, and above, 160 Gy (Fig 5-1). Furthermore, the elevated temperature post-IR IRSL signals at

200, 250 and 300°C, all yield stored dose estimates that continue to grow linearly to doses in excess of 160 Gy.

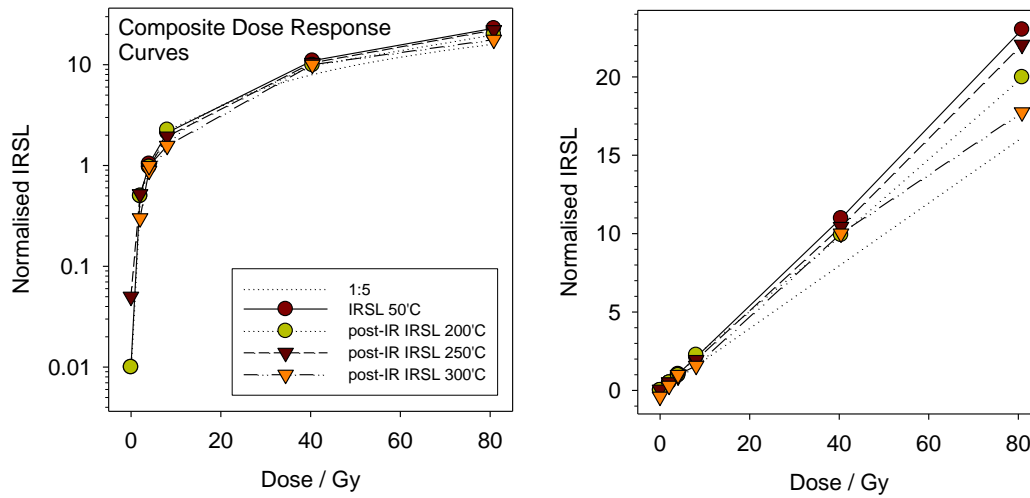


Figure 5-1: Composite dose responses for the IRSL signal at 50°C, and the equivalent MET post-IR IRSL signals at 200°C, 250°C and 300°C

Table 5-4 lists the stored dose estimates obtained following the preliminary SAR OSL and IRSL analyses on the paired quartz and K feldspar aliquots. On the basis of these results, the Chepnyalil samples - SUTL2614, 2616 and 2617, the Leopards Cave samples - SUTL2619 and 2620, and the Kiptogot samples - SUTL2621, 2622, 2624 and 2626-2627 can all potentially be dated by the conventional quartz SAR procedure; for the remaining samples, it would be necessary to examine different dating signals in quartz and feldspar, to determine the correct dating protocol. The samples approved for dating are all suitable for conventional quartz SAR analysis.

	Quartz OSL SAR stored dose / Gy		K feldspar IRSL SAR stored dose /Gy	K feldspar post-IR IRSL SAR stored dose /Gy
Chepnyalil Cave				
2612	>75-80			
2613	>75-80	103	118 ± 25 (18)	104 ± 2 (1.5)
2614	40 ± 4 (0.1)		121 ± 31 (22)	164 ± 52 (37)
2615	>75-80	160	163 ± 42 (29)	194 ± 44 (31)
2616	4.1 ± 0.4 (0.1)		0.3 ± 0.9 (0.7)	17 ± 7 (4.6)
2617	24 ± 13 (7)		37 ± 39 (28)	37 ± 24 (17)
2618	>75-80	82	58 ± 31 (22)	53 ± 7 (5.1)
Leopards Cave (Lower Chepnyalil Cave)				
2619	8.1 ± 0.1 (0.1)		5.1 ± 4.8 (3.4)	11 ± 14 (10)
2620	50 ± 18 (13)		5.6 ± 0.7 (0.5)	
Kiptogot Cave				
2621	3.6 ± 3.1 (2.2)		3.8 ± 0.5 (0.3)	4.5 ± 4.7 (3.3)
2622	12 ± 6 (4)		48 ± 26 (19)	45 ± 13 (9)
2623	>75-80	73	163 ± 34 (24)	122 ± 30 (21)
2624	35 ± 14 (9.9)			
2625	>75-80		261 ± 66 (47)	167 ± 33 (23)
2626	3 ± 2 (2)		13.8 ± 13.7	74 ± 72 (51)

			(9.7)	
2627	15 ± 2 (1)		38 ± 17 (12)	122 ± 5 (4)

Table 5-4: Quartz OSL SAR /K feldspar IRSL SAR/post-IR IRSL at 300°C stored dose estimates

* The OSL SAR dose response curves (see Appendix C) show saturation at doses >75-80 Gy at signal levels which are systematically lower than the natural OSL ratios. Figures D-1 to D-16 examine the dose response up to 160 Gy, indicating a possibility of a slight upward progression beyond the limit of exponential saturation (the stored dose value in italics indicates that a single aliquot from this sample did yield a normalised OSL value below the saturation dose)

5.3.3. Quartz SAR OSL determinations

Preheat plateau. To investigate the thermal stability of the OSL signal, the dependence of equivalent dose on preheat temperature was investigated, using various preheats (200, 220, 240 and 260 °C). The same thermal treatment was used for the natural/regeneration doses and the test doses. Representative plateau plots are shown in figure 5-3.

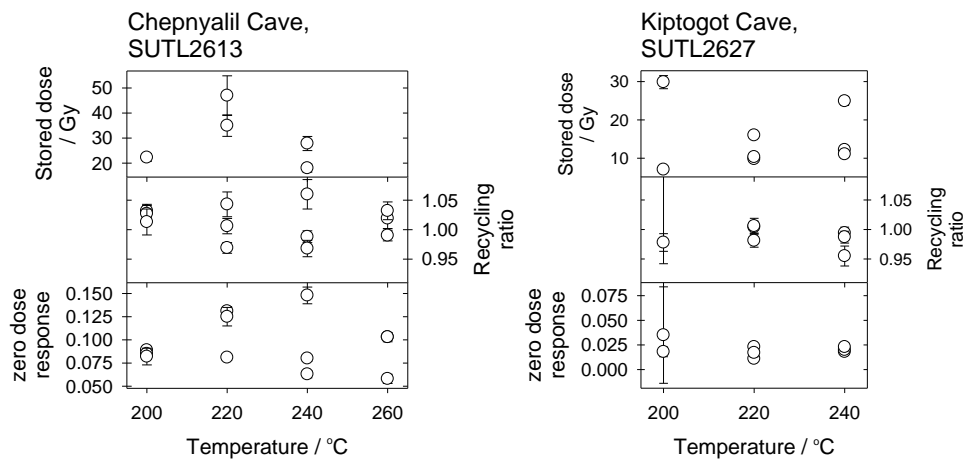


Figure 5-2: Preheat plateaus for SUTL2613 and SUTL2627

Note that there is no evidence of significant differences in the zero dose response, recycling ratio, or normalised OSL ratios (both in natural and regenerated dose points) between the sub-sets of discs pre-heated from 200°C to 260°C.

Thermal stability. To further examine the thermal stability of the natural and regenerative OSL and IRSL signals, pulsed annealing experiments were undertaken on the K feldspar extracts from SUTL2439 and 2440 (Fig. 5-4), and quartz extracts from SUTL2621 and 2623 (Fig. 5-5). The IRSL and OSL signals were recorded, using short stimulations (1 sec at 10% power, to minimise signal depletion), at a range of temperatures: 0 (Natural), 100, 125, 150, 175, 200, 210, 220, 230, 240, 250, 260, 270, 280, 290, 300, 310, 320, 330, 340, 350, 375, 400, 425°C. The experiment was repeated following a nominal dose of 100 Gy.

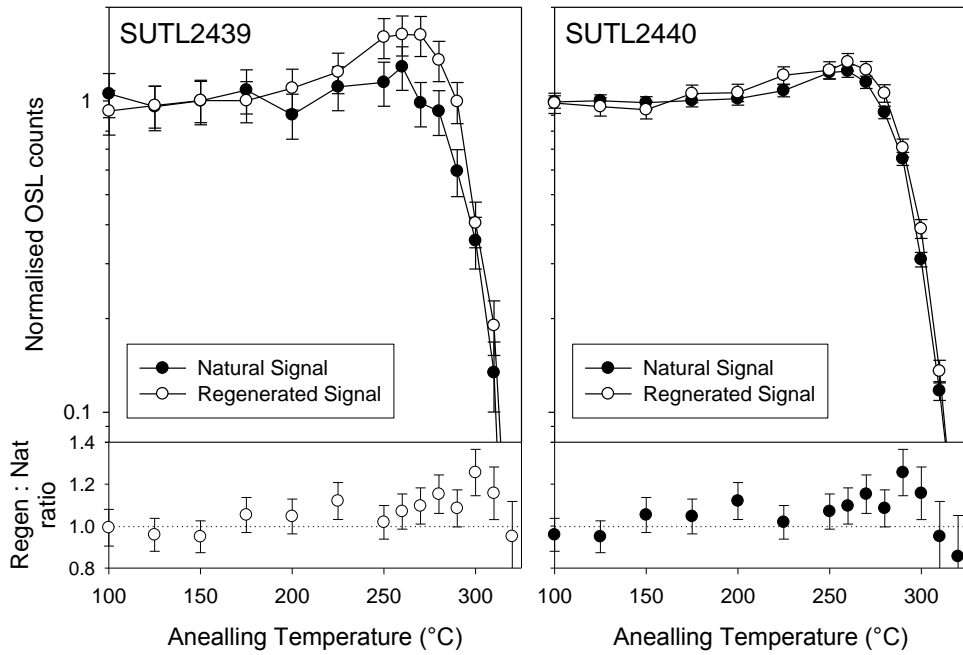


Figure 5-3: Pulsed annealing plots for the K feldspars extracts from SUTL2439 and 2440

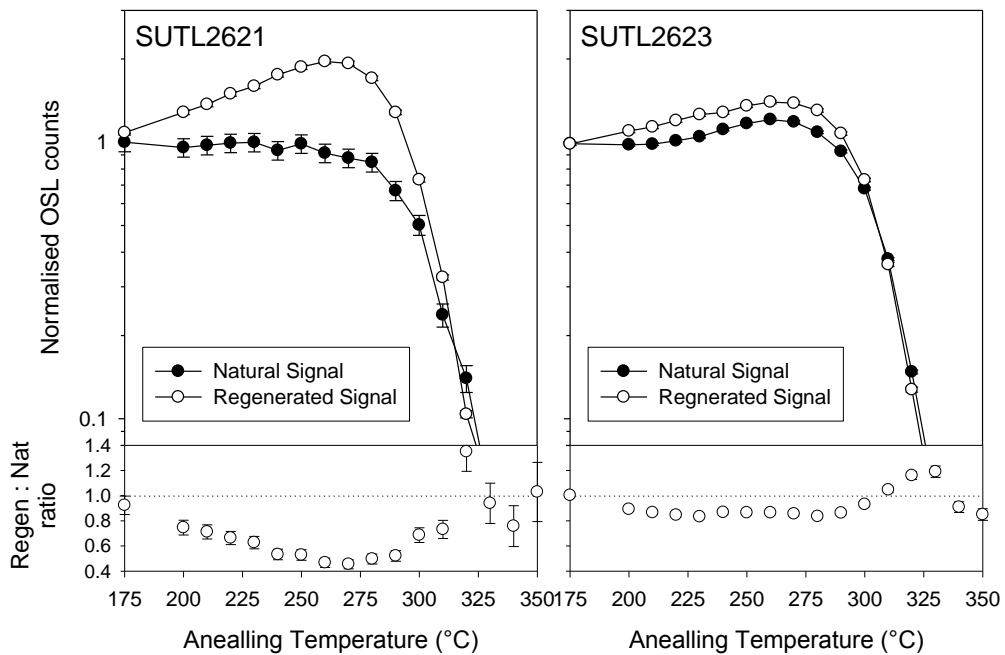


Figure 5-4: Pulsed annealing plots for the quartz extracts from SUTL2621 and 2623.

Figure 5-4 illustrates the response of the natural (black circles) and regenerated IRSL 50°C signals (white circles) from the K feldspar extracts to pulsed annealing. The natural and regenerated signals are normalised to the response of the first four aliquots. For the regenerated IRSL at 50°C, there is a minor reduction in signal intensity between c.100 and 250°C, and a rapid reduction between 250 and 350°C, such that most of the signal has been removed by 350°C. Kinnaird et al. (2012) showed that the elevated temperature post-IR IRSL signals reduced more slowly

through the temperature range 250 to 350°C than the equivalent IRSL signals. Figure 5-5 illustrates the response of the natural (black circles) and regenerated OSL signals (white circles) from quartz to pulsed annealing.

Signal component analysis. LM-OSL measurements were undertaken on quartz extracts from SUTL2439 and 2440 to identify the different constituent components of the luminescence signal, and track variations in these signals through the SAR sequence. LM-OSL measurements were made by linearly ramping the optical stimulation source, from zero to 90% power over a period of 3600 s. The OSL measurement was made at 125°C, with 60% power for 60 s. LM-OSL measurements were taken during readout of the natural signal, and then following (i) a 280°C preheat; (ii) irradiation to 10 Gy; (iii) an irradiation/preheat cycle; and (iv) a irradiation/preheat/OSL cycle (Fig. 5-6).

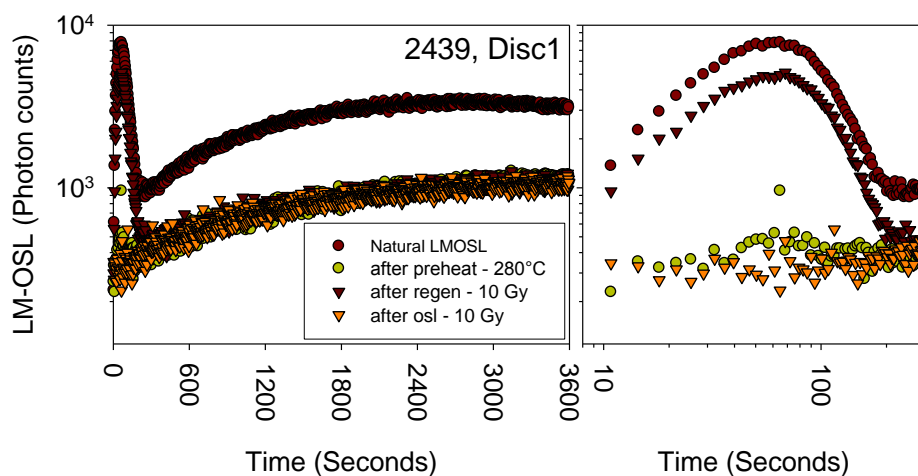


Figure 5-5: Linearly-modulated (LM)-OSL curves obtained for sample SUTL2349, during natural readout, preheat, irradiation, and irradiation/preheat/readout cycles

The LM-OSL curve obtained for the natural signal contains a sharp peak in the initial stages (< 100 seconds), followed by a broad, less intense peak in the later stages (> 100 seconds; Fig. 5-6). The sharp peak in the initial stages is identified as the easy to bleach or fast-decaying component of the quartz CW-OSL signal. The broad peak under higher stimulation powers corresponds to the medium and slow components. Therefore, the OSL signal of the Chepnyalil quartz appears to be dominated by its fast component. Large variations in brightness/sensitivity are apparent between the LM-OSL curves obtained following preheating to 280°C, irradiation to 5 Gy and the preheating/irradiating cycle.

Single aliquot equivalent dose distributions. For equivalent dose determination, data from single aliquot regenerative dose measurements were analysed using the Risø TL/OSL Viewer programme to export integrated summary files that were analysed in MS Excel and SigmaPlot. Composite dose response curves were constructed from selected discs and for each of the four preheating groups from each sample, and used to estimate equivalent dose values for each individual disc and their combined sets. Dose response curves for each of the four preheating temperature groups and the

combined data were determined using an exponential fit (Appendix D). The equivalent dose was then determined for each aliquot using the corresponding exponential fit parameters.

The distribution in equivalent dose values was examined using radial plotting methods. All samples revealed some heterogeneity in their equivalent dose distributions. Single aliquots were rejected from further analysis based on the test dose sensitivity check, SAR criteria checks, the robust mean, feldspar contamination and radial plots. Table 5-5 summarises the quality evaluation checks on the SAR data (once filtered); the mean sensitivity of each aliquot and sensitivity change, the recycling ratio and zero dose response.

SUTL No.	Sensitivity (counts/Gy)	Sensitivity change (%)	Recycling Ratio	Zero Dose (Gy)	IRSL response (%)
2612	16316 ± 7126	-0.64 ± 0.01	0.99 ± 0.02	0.21 ± 0.15	0.03 ± 0.02
2613	14000 ± 3516	0.44 ± 0.01	1.01 ± 0.02	0.26 ± 0.23	0.07 ± 0.07
2620	7475 ± 1717	-1.21 ± 0.01	0.95 ± 0.01	0.18 ± 0.23	-0.07 ± 0.07
2626	10979 ± 2947	-0.32 ± 0.01	0.97 ± 0.01	0.10 ± 0.09	0.04 ± 0.03
2627	16657 ± 3245	0.05 ± 0.01	1.00 ± 0.01	0.03 ± 0.01	1.04 ± 1.03

Table 5-5: Quartz SAR OSL quality parameters. Standard errors given.

5.3.1. Age determinations

The total dose rate is determined from the sum of the equivalent beta and gamma dose rates, and the cosmic dose rate. Age estimates are determined by dividing the equivalent stored dose by the dose rate. Uncertainty on the age estimates is given by combination of the uncertainty on the dose rates and stored doses, with an additional 5% external error. Table 5-6 lists the total dose rate, stored dose and corresponding age of the sample.

SUTL No.	Dose Rate / mGy a ⁻¹	Stored Dose / Gy	Years BP
2612	3.83 ± 0.19	>75-80	> 20 ka*
2613	3.55 ± 0.21	20.73 ± 0.40	5.84 ± 0.37
2620	2.34 ± 0.12	15.71 ± 0.35	6.72 ± 0.36
2626	3.25 ± 0.15	0.61 ± 0.01	0.19 ± 0.01
2627	2.45 ± 0.13	11.3 ± 0.14	4.62 ± 0.25

Table 5-6: Total dose rates, stored dose and age estimates

6. Discussion and conclusions

Multiple luminescence methods, from initial luminescence screening using portable OSL equipment, through laboratory characterisation measurements, to full quartz OSL SAR dating and polymineral IRSL SARA dating, have been successfully applied to a number of sediment stratigraphies at Chepnyalil and Kiptogot Cave. The key findings from each of these stages are reiterated here.

The field profiling was extremely informative. 76 samples were measured in the field, from 8 sediment profiles, across 3 sites, at Chepnyalil Cave, Leopards Cave and Kiptogot Cave. In general the sediment stratigraphies consistently encompassed a range of lithological units, from bedrock up, (i) a compacted, red-brown clayey loam, which enclosed the main lithic assemblage, (ii) a more poorly consolidated, red brown clayey loam, largely devoid of artefacts, and (iii) then various grey to brown loams, progressing upwards into grey, very loose topsoils. At Chepnyalil, the upper 10-20cms of the sedimentary profile, contains a range of heated materials, including reddened/fired earth, and ash. Each stratigraphic package could be distinguished on the basis of its luminescence proxy characteristics; for example, the compacted clays at the base of the succession, are characterised by large net IRSL and OSL signal intensities several orders of magnitude larger than those observed in the overlying deposits. Furthermore, through reference to independent age controls, it was possible to place the Chepnyalil Cave stratigraphies into a relative chronological sequence, and furthermore, correlate discrete packages of sediment between the lower and upper Chepnyalil caves and more tentatively, between Chepnyalil and Kiptogot.

Subsequently, laboratory profiling confirmed the correlations suggested in the field profiling dataset. Furthermore, the laboratory profiling results from the lower and upper units (ii and iii, above) at Chepnyalil and Kiptogot, confirmed a significant step in stored dose values across this lithological boundary (2-3 Gy vs 18 Gy and above), consistent with a notable unconformity, and a multiphase occupation of the caves. Additionally, the calibrated luminescence screening results, indicated the dating samples which could be potentially dated by the conventional quartz SAR OSL approach, and those that would require higher temperature quartz and K feldspar approaches.

Finally, the quartz SAR OSL ages, and the preliminary K feldspar post-IR elevated temperature IRSL, provide the means to construct sediment-OSL chronologies for the stratigraphies at Chepnyalil and Kiptogot, verifying that the lower units at these sites (enclosing the lithic assemblages which resemble MSA and LSA technologies) do contain strata of LSA age, if not earlier. It must be noted that full quantitative luminescence dating was restricted to five samples: two from the stratigraphically lower sequences at Chepnyalil, one from Leopards Cave, and two from the Kiptogot. Four of the samples produced finite ages in the range 5.8 ± 0.4 ka (SUTL2613), 6.7 ± 0.4 ka (SUTL2620), 4.6 ± 0.3 ka (SUTL2626), and AD 1830 ± 10 . The remaining sample showed natural luminescence signals in excess of the saturation signals for the regenerative dose curves. A minimum age estimate for this sample is in excess of 20 ka.

Table 6-1 lists the independent age controls that are present for the Chepnyalil and Kiptogot Caves, including radiocarbon ages received post-excavation. There is a good agreement between the sediment depositional ages listed here, the independent sediment depositional ages from Chepnyalil, and the inferred sediment ages at Chepnyalil and Kiptogot from the radiocarbon dates.

Method	Locality	Sample no.	Context	Age estimate
OSL	Chepnyalil, Upper Cave, Test Pit 1	Sample 2995	Level 99.89; 11 cm beneath ground surface	15.4 ± 4.1 ka (before 2011)
		Sample 2984	Level 99.26; 74 cm beneath surface	23.2 ± 2.4 ka
Radiocarbon	Leopard Cave, Test Pit 1	Beta-307191	45 cm beneath cave floor	1680 ± 30 yrs BP; cal AD 260-290 and 320-420
	Leopard Cave, Test Pit 2	SUERC-51768	120 to 140 cm beneath cave floor	15, 305 ± 49 yrs BP; cal BC 16,708 to 16,565
	Leopard Cave 'waterfall'	SUERC-51772	55 cm beneath cave floor, charcoal from top of layer	1796 ± 30 yrs BP; cal AD 140-196 or 208-255 or 300-327
	Chepnyalil, Upper Cave, Test Pit 2	Beta-307192	Level 98.56; 141 cm beneath ground surface	480 ± 30 yrs BP; cal AD 1410 to 1450
	Kiptogot Cave, Test Pit 4	SUERC-51767	Level 97.00;	203 ± 33 yrs BP; cal AD 1655-1680 or 1764-1804 or 1939-

Table 6-1: Independent age estimates for the sediment stratigraphies at Chepnyalil and Kiptogot, including new radiocarbon assays completed post-fieldwork

Having established a robust, relative chronology for the sediment stratigraphies using the portable OSL equipment, coupled with field gamma spectrometry, and having subsequently, verified these field relationships through calibrated luminescence measurements in the laboratory, it is highly tempting to expand our working sediment-OSL chronologies to include the preliminary age estimates reported above.

Earlier luminescence investigations (Kinnaird et al., 2012) on Chepnyalil sediment have shown that conventional quartz OSL SAR protocols are suitable to date strata younger than 15-20 ka, equivalent to a stored dose of 75-80 Gy, and that higher temperature quartz and post-IR IRSL K feldspar approaches are suitable for older strata, with doses continuing to grow up to and beyond 160 Gy.

Table 5-4 lists the stored dose estimates obtained for all 16 full dating samples by both quartz OSL SAR and K feldspar IRSL SAR/post-IR IRSL. In the Chepnyalil environmental setting, the quartz stored dose values, correspond to luminescence ages between 200 yrs BP and 25 ka BP, providing further confirmation of a prolonged environmental chronology, suggesting a complex, multiphase occupational history. Similarly, at Kiptogot, the range in quartz stored dose values, is consistent in a range of luminescence ages between 200 yrs BP and 25 ka. Note though, that for the lower units, the conventional quartz OSL SAR approach, returns normalised natural OSL values that are near to, or above the saturation limit in the dose response curve. For these samples, the IRSL/post-IRSL SAR approaches, and the IRSL SARA approach, potentially provide a better estimation of the true burial age. Future work will address the stability of these signals over prolonged storage periods.

6.1. Future work

The work conducted so far as been restricted to five samples out of the sample set of sixteen.

7. Acknowledgements

This research was made possible through the generous financial support of Mr. Peter Powles and his nephew Stephen Powles. The National Museums and Kenya Wildlife Services allowed the first author (TK) to carry out the research by giving him the permits both to carry out archaeological research as well as to carry out work inside the National Park.

8. References

- Nkirote, F. 2012. Report on the Pottery from Chepnyalil Rock Shelter, Mt Elgon. *National Museums of Kenya, Archaeological Report*
- Kiura, P. 2012. Preliminary archaeological research, Nov 2007, Mt Elgon National Park Caves. *National Museums of Kenya, Archaeological Report*
- Adamiec, G., Bailey, R.M., Wang, X.L., and Wintle, A.G., 2008, The mechanism of thermally transferred optically stimulated luminescence in quartz: *Journal of Physics D: Applied Physics*, v. 41, p. 135503.
- Adamiec, G., Duller, G.A.T., Roberts, H.M., and Wintle, A.G., 2010, Improving the TT-OSL SAR protocol through source trap characterisation: *Radiation Measurements*, v. 45, p. 768-777.
- Aitken, M.J., 1983, Dose rate data in SI units: *PACT*, v. 9, p. 69–76.
- Alexander, S.A., 2007, The stability of the remnant luminescence emissions of alkali feldspar [unpublished PhD thesis thesis]: Glasgow, University of Glasgow.
- Bailey, R.M., 1998, The form of the optically stimulated luminescence signal of quartz: implications for dating.: London, Unpublished Ph.D. Thesis, University of London.
- Bøtter-Jensen, L., Bulur, E., Duller, G.A.T., and Murray, A.S., 2000, Advances in luminescence instrument systems: *Radiation Measurements*, v. 32, p. 523-528.
- Burbidge, C.I., Sanderson, D.C.W., Housley, R.A., and Allsworth Jones, P., 2007, Survey of Palaeolithic sites by luminescence profiling, a case study from Eastern Europe: *Quaternary Geochronology*, v. 2, p. 296-302.
- Buylaert, J.P., Murray, A.S., Thomsen, K.J., and Jain, M., 2009, Testing the potential of an elevated temperature IRSL signal from K-feldspar: *Radiation Measurements*, v. 44, p. 560-565.
- Duller, G.A.T., and Wintle, A.G., 2011, A review of the thermally transferred optically stimulated luminescence signal from quartz for dating sediments: *Quaternary Geochronology*.
- Huntley, D.J., 2006, An explanation of the power-law decay of luminescence: *Journal of Physics: Condensed Matter*, v. 18, p. 1359.
- Huntley, D.J., Baril, M.R., and Haidar, S., 2007, Tunnelling in plagioclase feldspars: *Journal of Physics D: Applied Physics*, v. 40, p. 900.

- Huntley, D.J., Godfrey-Smith, D.I., and Thewalt, M.L.W., 1985, Optical dating of sediments: *Nature*, v. 313, p. 105-107.
- Huntley, D.J., and Lamothe, M., 2001, Ubiquity of anomalous fading in K-feldspars and the measurement and correction for it in optical dating: *Canadian Journal of Earth Sciences*, v. 38, p. 1093-1106.
- Kiura, P. 2012. Preliminary archaeological research, Nov 2007, Mt Elgon National Park Caves. *National Museums of Kenya, Archaeological Report*
- Krbetschek, M.R., Götze, J., Dietrich, A., and Trautmann, T., 1997, Spectral information from minerals relevant for luminescence dating: *Radiation Measurements*, v. 27, p. 695-748.
- Krbetschek, M.R., and Rieser, U., 1995, Luminescence spectra of alkalifeldspars and plagioclases: *Radiation Measurements*, v. 24, p. 473-477.
- Mejdahl, V., 1979, Thermoluminescence daing: Beta-dose attenuation in quartz grains *Archaeometry*, v. 21, p. 61-72.
- Mejdahl, V., and Bøtter-Jensen, L., 1994, Luminescence dating of archaeological materials using a new technique based on single aliquot measurements: *Quaternary Science Reviews*, v. 13, p. 551-554.
- , 1997, Experience with the SARA OSL method: *Radiation Measurements*, v. 27, p. 291-294.
- Murray, A.S., and Wintle, A.G., 2000, Luminescence dating of quartz using an improved single-aliquot regenerative-dose protocol: *Radiation Measurements*, v. 32, p. 57-73.
- NEA, 2000, The JEF-2.2 Nuclear Data Library: Nuclear Energy Agency, Organisation for economic Co-operation and Development. *JEFF Report*, v. 17.
- Nkirote, F. 2012. Report on the Pottery from Chepnyalil Rock Shelter, Mt Elgon. *National Museums of Kenya, Archaeological Report*
- Pagonis, V., Wintle, A.G., Chen, R., and Wang, X.L., 2008, A theoretical model for a new dating protocol for quartz based on thermally transferred OSL (TT-OSL): *Radiation Measurements*, v. 43, p. 704-708.
- Prescott, J.R., and Hutton, J.T., 1994, Cosmic ray contributions to dose rates for luminescence and ESR dating: Large depths and long-term time variations: *Radiation Measurements*, v. 23, p. 497-500.
- Sanderson, D.C.W., 1987, Thermoluminescence dating of vitrified Scottish Forts: Paisley, Paisley college.
- , 1988a, Fading of thermoluminescence in feldspars: Characteristics and corrections: *International Journal of Radiation Applications and Instrumentation. Part D. Nuclear Tracks and Radiation Measurements*, v. 14, p. 155-161.
- , 1988b, Thick source beta counting (TSBC): A rapid method for measuring beta dose-rates: *International Journal of Radiation Applications and Instrumentation. Part D. Nuclear Tracks and Radiation Measurements*, v. 14, p. 203-207.
- Sanderson, D.C.W., Bishop, P., Houston, I., and Boonsener, M., 2001, Luminescence characterisation of quartz-rich cover sands from NE Thailand: *Quaternary Science Reviews*, v. 20, p. 893-900.
- Sanderson, D.C.W., Bishop, P., Stark, M.T., and Spencer, J.Q., 2003, Luminescence dating of anthropogenically reset canal sediments from Angkor Borei, Mekong Delta, Cambodia: *Quaternary Science Reviews*, v. 22, p. 1111-1121.
- Sanderson, D.C.W., and Murphy, S., 2010, Using simple portable OSL measurements and laboratory characterisation to help understand complex and heterogeneous

- sediment sequences for luminescence dating: *Quaternary Geochronology*, v. 5, p. 299-305.
- Spooner, N.A., 1992, Optical dating: Preliminary results on the anomalous fading of luminescence from feldspars: *Quaternary Science Reviews*, v. 11, p. 139-145.
- , 1994, The anomalous fading of infrared-stimulated luminescence from feldspars: *Radiation Measurements*, v. 23, p. 625-632.
- Thiel, C., Buylaert, J.-P., Murray, A., Terhorst, B., Hofer, I., Tsukamoto, S., and Frechen, M., 2011, Luminescence dating of the Stratzing loess profile (Austria) – Testing the potential of an elevated temperature post-IR IRSL protocol: *Quaternary International*, v. 234, p. 23-31.
- Thomsen, K.J., Murray, A.S., Jain, M., and Bøtter-Jensen, L., 2008, Laboratory fading rates of various luminescence signals from feldspar-rich sediment extracts: *Radiation Measurements*, v. 43, p. 1474-1486.
- Tsukamoto, S., Duller, G.A.T., and Wintle, A.G., 2008, Characteristics of thermally transferred optically stimulated luminescence (TT-OSL) in quartz and its potential for dating sediments: *Radiation Measurements*, v. 43, p. 1204-1218.
- Visocekas, R., Spooner, N.A., Zink, A., and Blanc, P., 1994, Tunnel afterglow, fading and infrared emission in thermoluminescence of feldspars: *Radiation Measurements*, v. 23, p. 377-385.
- Visocekas, R., Tale, V., Zink, A., and Tale, I., 1998, Trap spectroscopy and tunnelling luminescence in feldspars: *Radiation Measurements*, v. 29, p. 427-434.
- Wang, X.L., Wintle, A.G., and Lu, Y.C., 2006, Thermally transferred luminescence in fine-grained quartz from Chinese loess: Basic observations: *Radiation Measurements*, v. 41, p. 649-658.
- Wintle, A.G., 1973, Anomalous Fading of Thermo-luminescence in Mineral Samples: *Nature*, v. 245, p. 143-144.
- Zink, A., Visocekas, R., and Bos, A.J.J., 1995, Comparison of 'blue' and 'infrared' emission bands in thermoluminescence of alkali feldspars: *Radiation Measurements*, v. 24, p. 513-518.

Appendix A: Chemical analysis of soil samples from Chepnyalil cave

Table A-1: Chemical analysis of soil samples from Chepnyalil using the atomic absorption spectrophotometer method. *Department of Mines & Geology, University of Nairobi*

Elements	Reference height in section, Test Pit 1, Chepnyalil Cave / cm					
	90-80	80-70	70-60	60-50	50-40	40-20
	Sample 1/ wt. %	Sample 2/ wt. %	Sample 3/ wt. %	Sample 4/ wt. %	Sample 5/ wt. %	Sample 6/ wt. %
SiO ₂	35.00	36.00	31.80	35.00	38.00	26.00
Al ₂ O ₃	12.40	14.40	12.40	14.01	10.80	12.57
CaO	5.19	6.46	12.60	7.86	7.74	16.20
MgO	2.15	1.87	2.44	1.35	1.46	1.67
Na ₂ O	0.51	0.53	0.75	0.65	0.95	0.91
K ₂ O	2.70	2.60	2.48	3.60	2.24	1.83
TiO ₂	3.34	4.69	2.60	2.50	2.46	1.73
MnO	0.28	0.33	0.26	0.50	0.25	0.20
Fe ₂ O ₃	15.3	14.50	7.10	25.0	15.40	9.80
P ₂ O ₅	-	-	6.00	1.80	4.40	11.0
LOI	22.82	18.27	20.34	8.00	16.45	17.15
Total	99.69	99.65	98.77	100.27	100.15	99.06

Table B-2: Mineral content identification for soil samples from Chepnyalil area using the X-ray diffraction method. *Department of Mines & Geology, University of Nairobi*

Sample No.	Minerals identified
1	Magnetite/ Hematite+ Montmorillonite + K-feldspar + Quartz (?)
2	Magnetite + Montmorillonite
3	Magnetite + Montmorillonite + Quartz
4	Magnetite/Hematite + Montmorillonite + K-feldspar
5	Magnetite/Hematite + Quartz + K-feldspar + Montmorillonite
6	Montmorillonite + Magnetite + Apatite + Quartz (?)

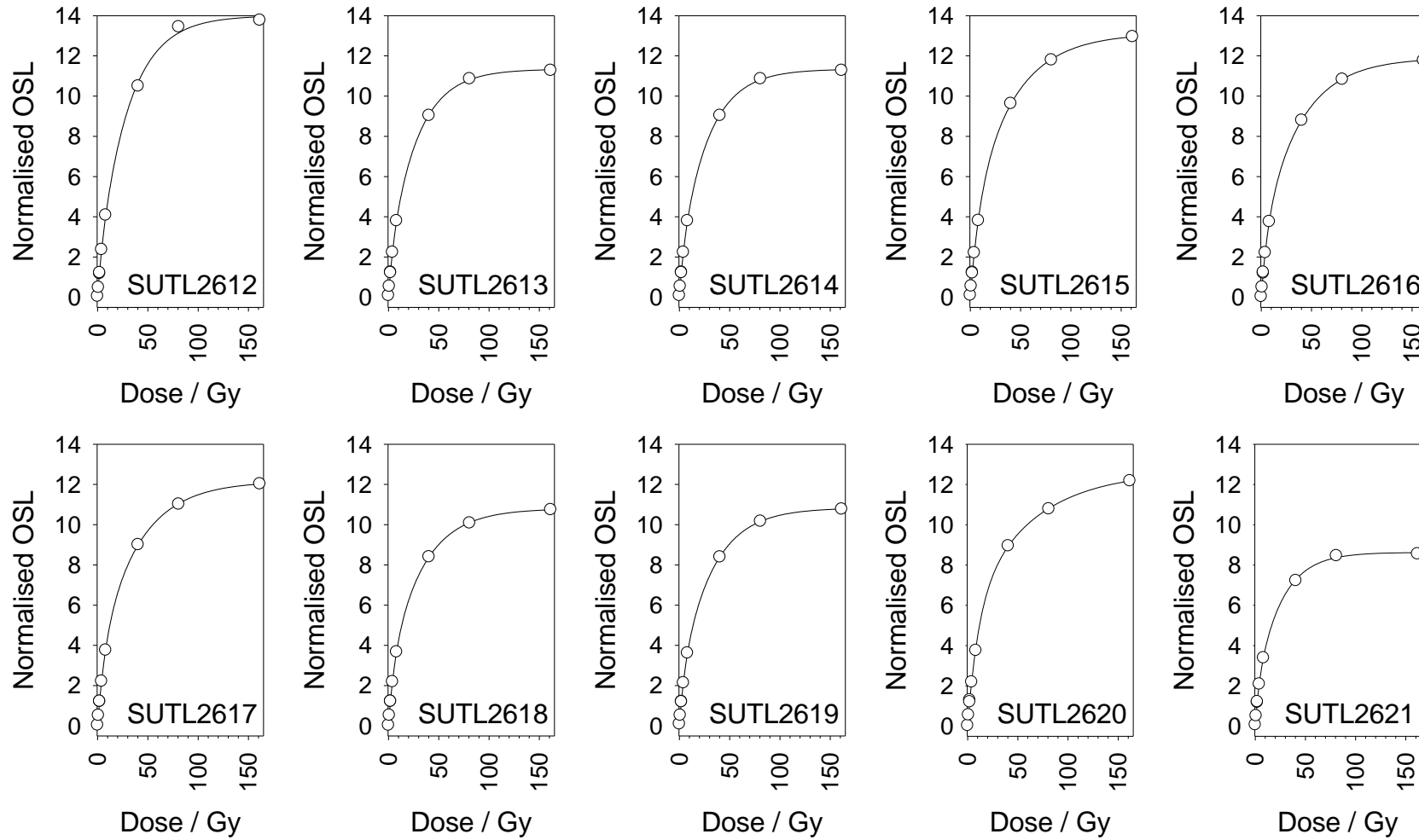
Appendix B: Luminescence Field Profiling Results

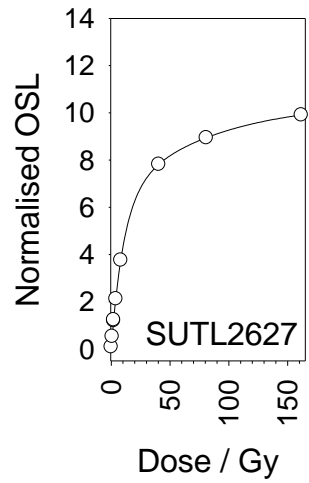
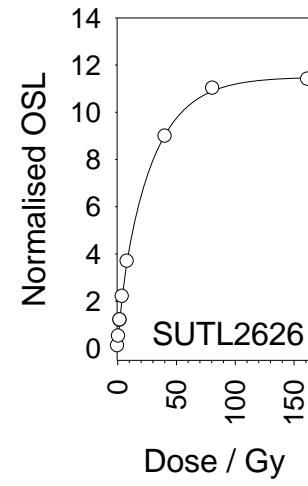
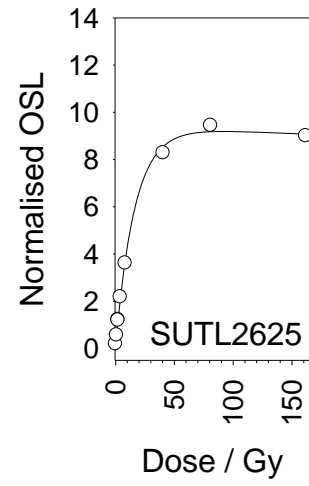
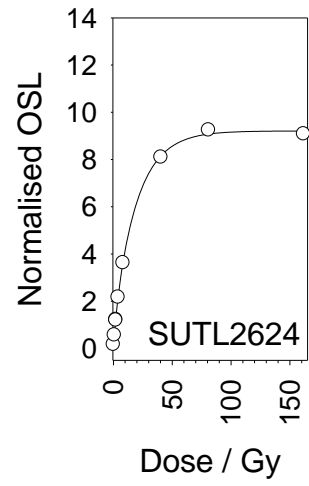
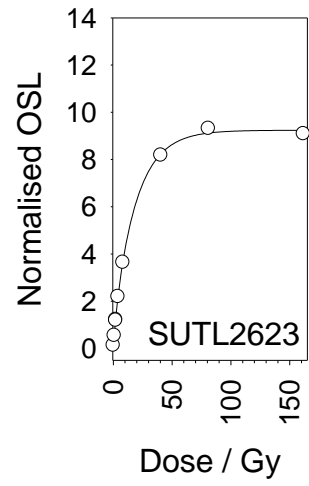
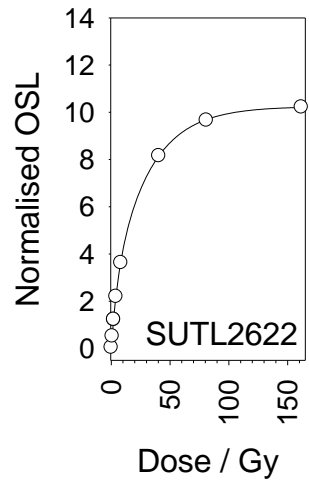
Table B-1: Portable OSL data from Chepnyalil Cave, 10-15th October 2013

Field no.	Red Net signal intensity	Depletion ratio	Blue Net signal intensity	Depletion ratio	IRSL : OSL ratio
Profile 1: Upper Chepnyalil Cave, Test Pit 1, southern profile					
P1/1	611 ± 58	1.16 ± 0.08	14847 ± 132	2.69 ± 0.05	0.041 ± 0.004
P1/2	4765 ± 86	1.36 ± 0.04	49957 ± 230	2.13 ± 0.02	0.095 ± 0.002
P1/3	11980 ± 120	1.37 ± 0.03	103213 ± 325	2.06 ± 0.01	0.116 ± 0.001
P1/4	20154 ± 151	1.40 ± 0.02	143656 ± 383	2.05 ± 0.01	0.140 ± 0.001
P1/5	21693 ± 156	1.41 ± 0.02	151207 ± 393	1.91 ± 0.01	0.143 ± 0.001
P1/6	23884 ± 162	1.43 ± 0.02	148560 ± 390	1.91 ± 0.01	0.161 ± 0.001
P1/7	19298 ± 148	1.39 ± 0.02	140064 ± 379	1.94 ± 0.01	0.138 ± 0.001
P1/8	18200 ± 144	1.43 ± 0.02	121106 ± 352	2.02 ± 0.01	0.150 ± 0.001
P1/9	17881 ± 143	1.38 ± 0.02	121970 ± 353	1.96 ± 0.01	0.147 ± 0.001
P1/10	30726 ± 182	1.38 ± 0.02	189908 ± 440	1.92 ± 0.01	0.162 ± 0.001
Profile 2: Upper Chepnyalil Cave, Test Pit 1, northern profile					
P2/1	3998 ± 78	1.33 ± 0.04	60634 ± 251	2.34 ± 0.02	0.066 ± 0.001
P2/2	7095 ± 99	1.28 ± 0.03	80251 ± 289	2.10 ± 0.02	0.088 ± 0.001
P2/3	10713 ± 115	1.31 ± 0.03	106997 ± 331	2.27 ± 0.02	0.100 ± 0.001
P2/4	8094 ± 102	1.39 ± 0.03	85788 ± 298	2.09 ± 0.02	0.094 ± 0.001
P2/5	9766 ± 110	1.36 ± 0.03	90887 ± 306	2.01 ± 0.01	0.107 ± 0.001
P2/6	12071 ± 120	1.35 ± 0.02	99340 ± 319	1.99 ± 0.01	0.122 ± 0.001
P2/7	10795 ± 114	1.36 ± 0.03	95152 ± 313	1.98 ± 0.01	0.113 ± 0.001
P2/8	9806 ± 110	1.33 ± 0.03	91862 ± 307	2.17 ± 0.02	0.107 ± 0.001
P2/9	12929 ± 123	1.37 ± 0.02	105407 ± 329	1.94 ± 0.01	0.123 ± 0.001
P2/10	18866 ± 145	1.42 ± 0.02	139552 ± 377	1.92 ± 0.01	0.135 ± 0.001
P2/11	13357 ± 125	1.34 ± 0.02	121949 ± 354	1.81 ± 0.01	0.110 ± 0.001
P2/12	2089 ± 66	1.25 ± 0.05	68218 ± 266	1.96 ± 0.02	0.031 ± 0.001
P2/13	2945 ± 72	1.33 ± 0.05	35158 ± 193	1.91 ± 0.02	0.084 ± 0.002
Profile 3: Upper Chepnyalil Cave, Test Pit 3					
P3/1			5710 ± 90	3.77 ± 0.13	
P3/2	118 ± 48	1.01 ± 0.12	3919 ± 78	3.36 ± 0.13	0.030 ± 0.012
P3/3	49 ± 50	1.25 ± 0.14	2963 ± 72	3.12 ± 0.14	0.017 ± 0.017
P3/4			3092 ± 72	3.38 ± 0.15	
P3/5			3544 ± 76	2.95 ± 0.12	
P3/6			4034 ± 80	3.08 ± 0.12	
P3/7			3538 ± 76	3.00 ± 0.12	
P3/8			3080 ± 74	2.81 ± 0.12	
Profile 4: Upper Chepnyalil Cave, Test Pit 2					
P4/1		1.05 ± 0.11	6466 ± 105	4.16 ± 0.14	
P4/2	128 ± 67	1.19 ± 0.12	8381 ± 114	3.89 ± 0.11	0.015 ± 0.008
P4/3		1.12 ± 0.14	11506 ± 125	3.45 ± 0.08	
P4/4		1.01 ± 0.13	9130 ± 116	3.54 ± 0.10	
P4/5	216 ± 65	1.06 ± 0.11	8497 ± 112	2.92 ± 0.08	0.025 ± 0.008
P4/6	101 ± 64	1.08 ± 0.13	8688 ± 113	3.80 ± 0.11	0.012 ± 0.007
P4/7		1.43 ± 0.19	7884 ± 109	4.12 ± 0.13	
P4/8	63 ± 63	0.83 ± 0.11	5828 ± 99	4.29 ± 0.16	0.011 ± 0.011
P4/9	135 ± 62	1.12 ± 0.15	5653 ± 97	3.93 ± 0.15	0.024 ± 0.011
P4/10	102 ± 62	0.83 ± 0.11	6133 ± 99	3.69 ± 0.13	0.017 ± 0.010
P4/11		1.14 ± 0.11	4691 ± 95	3.61 ± 0.14	
P4/12		1.39 ± 0.09	7177 ± 110	2.47 ± 0.07	

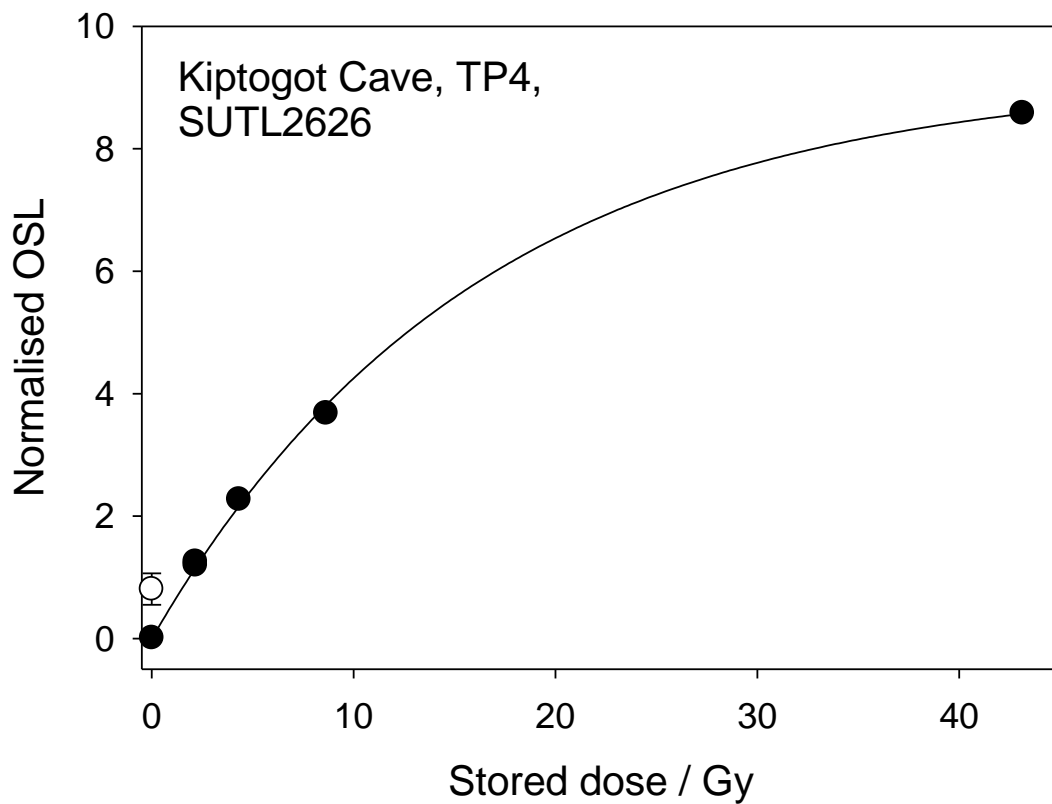
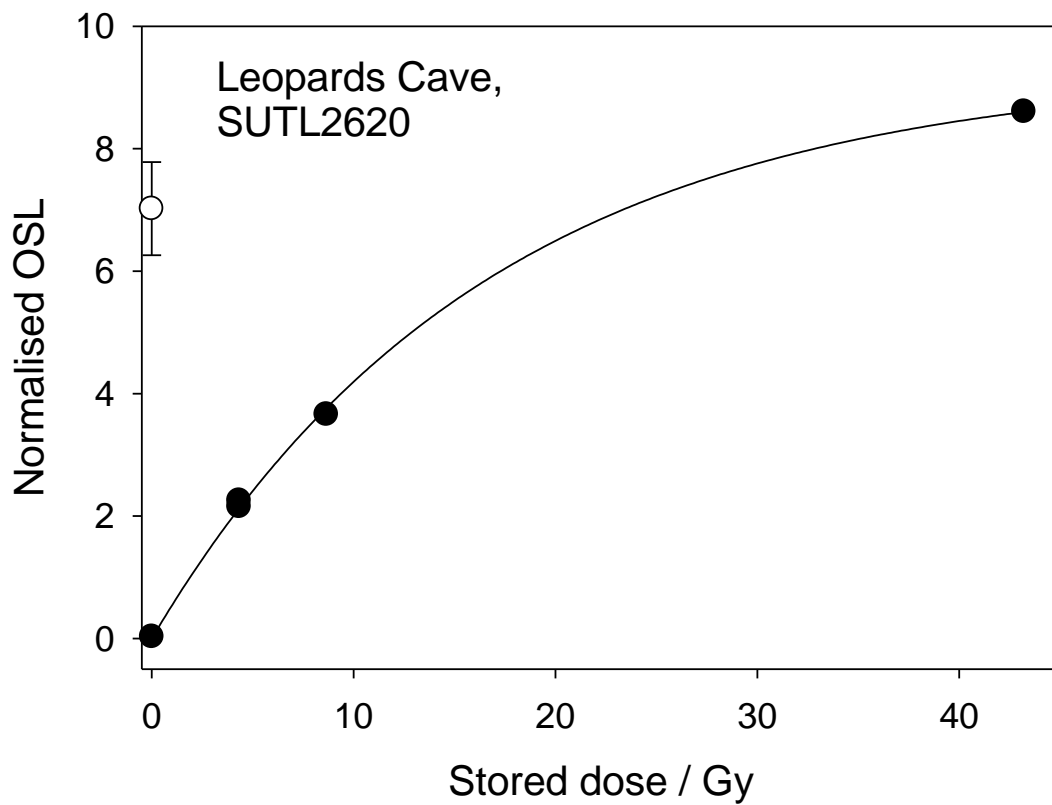
Profile 5: Lower Chepnyalil Cave (Leopards Cave); Test Pit 1					
P5/1		0.98 ± 0.13	2973 ± 84	1.94 ± 0.08	
P5/2	84 ± 66	1.05 ± 0.11	2140 ± 81	2.03 ± 0.10	0.039 ± 0.031
P5/3	80 ± 61	1.01 ± 0.15	3337 ± 85	2.37 ± 0.10	0.024 ± 0.018
P5/4	31 ± 62	1.06 ± 0.14	5226 ± 97	1.93 ± 0.06	0.006 ± 0.012
P5/5	185 ± 54	1.22 ± 0.13	7172 ± 100	1.72 ± 0.04	0.026 ± 0.007
P5/6	468 ± 58	1.02 ± 0.08	15907 ± 137	1.98 ± 0.03	0.029 ± 0.004
P5/7	284 ± 54	1.23 ± 0.12	9871 ± 112	1.78 ± 0.04	0.029 ± 0.005
P5/8	1061 ± 62	1.18 ± 0.07	60301 ± 251	2.03 ± 0.02	0.018 ± 0.001
P5/9	2625 ± 74	1.26 ± 0.05	95273 ± 313	1.98 ± 0.01	0.028 ± 0.001
P5/10	1999 ± 69	1.20 ± 0.05	103403 ± 326	2.09 ± 0.01	0.019 ± 0.001
P5/11	2605 ± 74	1.26 ± 0.05	85571 ± 297	1.91 ± 0.01	0.030 ± 0.001
P5/12	1372 ± 66	1.21 ± 0.06	80129 ± 288	1.98 ± 0.01	0.017 ± 0.001
Profile 6: Kiptogot Cave, eastern entrance; Test pit 1					
P6/1	4257 ± 88	1.30 ± 0.04	104461 ± 329	2.04 ± 0.01	0.041 ± 0.001
P6/2			170486 ± 416	2.07 ± 0.01	
P6/3			180855 ± 429	2.08 ± 0.01	
P6/4			175109 ± 422	1.96 ± 0.01	
P6/5			151230 ± 393	1.98 ± 0.01	
Profile 7: Kiptogot Cave, western entrance; Test Pit 3					
P7/1			4175 ± 83	2.05 ± 0.07	
P7/2			8000 ± 103	2.39 ± 0.06	
P7/3			6608 ± 95	2.44 ± 0.07	
P7/4			14258 ± 130	2.09 ± 0.04	
P7/5			37880 ± 202	2.12 ± 0.02	
P7/6			143725 ± 383	1.97 ± 0.01	
P7/7			189933 ± 440	1.95 ± 0.01	
P7/8			127308 ± 361	2.00 ± 0.01	
P7/9			233714 ± 487	2.26 ± 0.01	
P7/10			147999 ± 388	2.07 ± 0.01	
Profile 8: Kiptogot Cave; Test Pit 2					
P8/1			9702 ± 107	2.39 ± 0.05	
P8/2			8762 ± 102	2.08 ± 0.05	
P8/3			13218 ± 122	2.46 ± 0.05	
P8/4			117462 ± 346	2.00 ± 0.01	
P8/5			110163 ± 335	2.03 ± 0.01	
P8/6			159212 ± 402	2.02 ± 0.01	

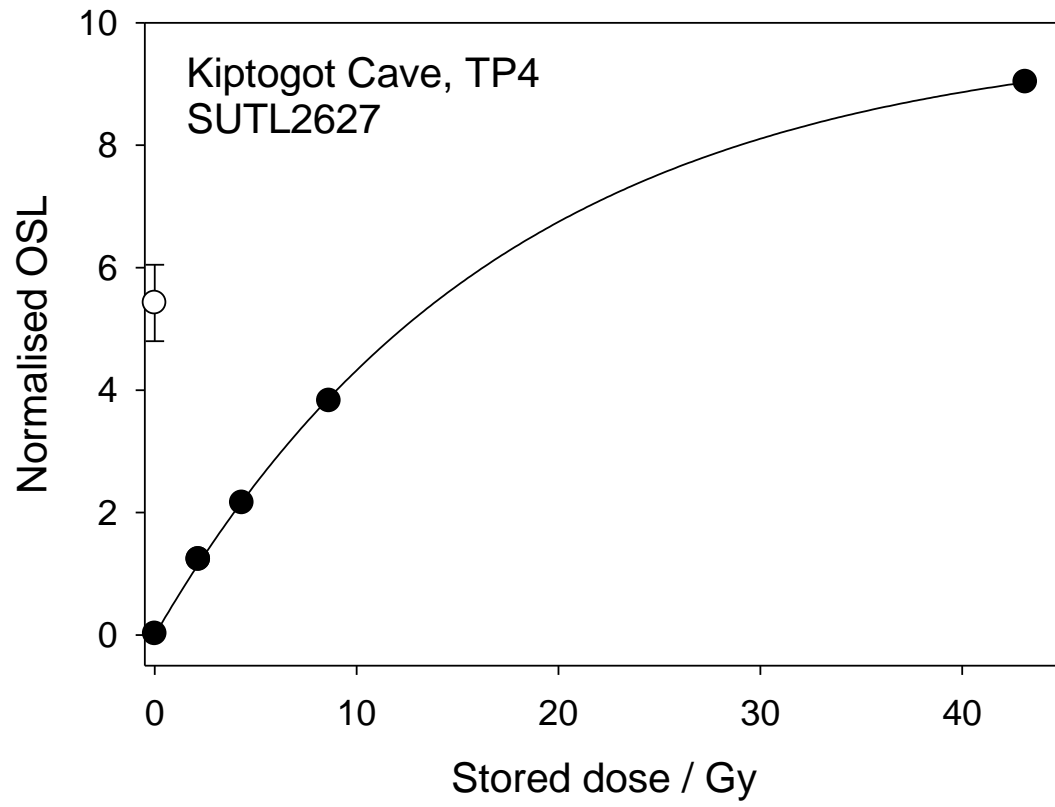
Appendix C: Calibrated luminescence screening measurements - composite dose response curves





Appendix D: Dose response curves





- Adamiec, G., Bailey, R.M., Wang, X.L., and Wintle, A.G., 2008, The mechanism of thermally transferred optically stimulated luminescence in quartz: *Journal of Physics D: Applied Physics*, v. 41, p. 135503.
- Adamiec, G., Duller, G.A.T., Roberts, H.M., and Wintle, A.G., 2010, Improving the TT-OSL SAR protocol through source trap characterisation: *Radiation Measurements*, v. 45, p. 768-777.
- Aitken, M.J., 1983, Dose rate data in SI units: *PACT*, v. 9, p. 69–76.
- Alexander, S.A., 2007, The stability of the remnant luminescence emissions of alkali feldspar [unpublished PhD thesis thesis]: Glasgow, University of Glasgow.
- Bailey, R.M., 1998, The form of the optically stimulated luminescence signal of quartz: implications for dating.: London, Unpublished Ph.D. Thesis, University of London.
- Bøtter-Jensen, L., Bulur, E., Duller, G.A.T., and Murray, A.S., 2000, Advances in luminescence instrument systems: *Radiation Measurements*, v. 32, p. 523-528.
- Burbidge, C.I., Sanderson, D.C.W., Housley, R.A., and Allsworth Jones, P., 2007, Survey of Palaeolithic sites by luminescence profiling, a case study from Eastern Europe: *Quaternary Geochronology*, v. 2, p. 296-302.
- Buylaert, J.P., Murray, A.S., Thomsen, K.J., and Jain, M., 2009, Testing the potential of an elevated temperature IRSL signal from K-feldspar: *Radiation Measurements*, v. 44, p. 560-565.
- Duller, G.A.T., and Wintle, A.G., 2011, A review of the thermally transferred optically stimulated luminescence signal from quartz for dating sediments: *Quaternary Geochronology*.
- Huntley, D.J., 2006, An explanation of the power-law decay of luminescence: *Journal of Physics: Condensed Matter*, v. 18, p. 1359.
- Huntley, D.J., Baril, M.R., and Haidar, S., 2007, Tunnelling in plagioclase feldspars: *Journal of Physics D: Applied Physics*, v. 40, p. 900.
- Huntley, D.J., Godfrey-Smith, D.I., and Thewalt, M.L.W., 1985, Optical dating of sediments: *Nature*, v. 313, p. 105-107.
- Huntley, D.J., and Lamothe, M., 2001, Ubiquity of anomalous fading in K-feldspars and the measurement and correction for it in optical dating: *Canadian Journal of Earth Sciences*, v. 38, p. 1093-1106.
- Krbetschek, M.R., Götze, J., Dietrich, A., and Trautmann, T., 1997, Spectral information from minerals relevant for luminescence dating: *Radiation Measurements*, v. 27, p. 695-748.
- Krbetschek, M.R., and Rieser, U., 1995, Luminescence spectra of alkalifeldspars and plagioclases: *Radiation Measurements*, v. 24, p. 473-477.
- Mejdahl, V., 1979, Thermoluminescence daing: Beta-dose attenuation in quartz grains *Archaeometry*, v. 21, p. 61-72.
- Mejdahl, V., and Bøtter-Jensen, L., 1994, Luminescence dating of archaeological materials using a new technique based on single aliquot measurements: *Quaternary Science Reviews*, v. 13, p. 551-554.
- , 1997, Experience with the SARA OSL method: *Radiation Measurements*, v. 27, p. 291-294.
- Murray, A.S., and Wintle, A.G., 2000, Luminescence dating of quartz using an improved single-aliquot regenerative-dose protocol: *Radiation Measurements*, v. 32, p. 57-73.
- NEA, 2000, The JEF-2.2 Nuclear Data Library: Nuclear Energy Agency, Organisation for economic Co-operation and Development. JEFF Report, v. 17.

- Pagonis, V., Wintle, A.G., Chen, R., and Wang, X.L., 2008, A theoretical model for a new dating protocol for quartz based on thermally transferred OSL (TT-OSL): *Radiation Measurements*, v. 43, p. 704-708.
- Prescott, J.R., and Hutton, J.T., 1994, Cosmic ray contributions to dose rates for luminescence and ESR dating: Large depths and long-term time variations: *Radiation Measurements*, v. 23, p. 497-500.
- Sanderson, D.C.W., 1987, Thermoluminescence dating of vitrified Scottish Forts: Paisley, Paisley college.
- , 1988a, Fading of thermoluminescence in feldspars: Characteristics and corrections: *International Journal of Radiation Applications and Instrumentation. Part D. Nuclear Tracks and Radiation Measurements*, v. 14, p. 155-161.
- , 1988b, Thick source beta counting (TSBC): A rapid method for measuring beta dose-rates: *International Journal of Radiation Applications and Instrumentation. Part D. Nuclear Tracks and Radiation Measurements*, v. 14, p. 203-207.
- Sanderson, D.C.W., Bishop, P., Houston, I., and Boonsener, M., 2001, Luminescence characterisation of quartz-rich cover sands from NE Thailand: *Quaternary Science Reviews*, v. 20, p. 893-900.
- Sanderson, D.C.W., Bishop, P., Stark, M.T., and Spencer, J.Q., 2003, Luminescence dating of anthropogenically reset canal sediments from Angkor Borei, Mekong Delta, Cambodia: *Quaternary Science Reviews*, v. 22, p. 1111-1121.
- Sanderson, D.C.W., and Murphy, S., 2010, Using simple portable OSL measurements and laboratory characterisation to help understand complex and heterogeneous sediment sequences for luminescence dating: *Quaternary Geochronology*, v. 5, p. 299-305.
- Spooner, N.A., 1992, Optical dating: Preliminary results on the anomalous fading of luminescence from feldspars: *Quaternary Science Reviews*, v. 11, p. 139-145.
- , 1994, The anomalous fading of infrared-stimulated luminescence from feldspars: *Radiation Measurements*, v. 23, p. 625-632.
- Thiel, C., Buylaert, J.-P., Murray, A., Terhorst, B., Hofer, I., Tsukamoto, S., and Frechen, M., 2011, Luminescence dating of the Stratzing loess profile (Austria) – Testing the potential of an elevated temperature post-IR IRSL protocol: *Quaternary International*, v. 234, p. 23-31.
- Thomsen, K.J., Murray, A.S., Jain, M., and Bøtter-Jensen, L., 2008, Laboratory fading rates of various luminescence signals from feldspar-rich sediment extracts: *Radiation Measurements*, v. 43, p. 1474-1486.
- Tsukamoto, S., Duller, G.A.T., and Wintle, A.G., 2008, Characteristics of thermally transferred optically stimulated luminescence (TT-OSL) in quartz and its potential for dating sediments: *Radiation Measurements*, v. 43, p. 1204-1218.
- Visocekas, R., Spooner, N.A., Zink, A., and Blanc, P., 1994, Tunnel afterglow, fading and infrared emission in thermoluminescence of feldspars: *Radiation Measurements*, v. 23, p. 377-385.
- Visocekas, R., Tale, V., Zink, A., and Tale, I., 1998, Trap spectroscopy and tunnelling luminescence in feldspars: *Radiation Measurements*, v. 29, p. 427-434.
- Wang, X.L., Wintle, A.G., and Lu, Y.C., 2006, Thermally transferred luminescence in fine-grained quartz from Chinese loess: Basic observations: *Radiation Measurements*, v. 41, p. 649-658.

- Wintle, A.G., 1973, Anomalous Fading of Thermo-luminescence in Mineral Samples: *Nature*, v. 245, p. 143-144.
- Zink, A., Visocekas, R., and Bos, A.J.J., 1995, Comparison of 'blue' and 'infrared' emission bands in thermoluminescence of alkali feldspars: *Radiation Measurements*, v. 24, p. 513-518.